The "Missing baryons"—what is it? Where is it? How much?

Yin-Zhe Ma (马寅哲)
University of KwaZulu-Natal, South Africa
(Adjunct Professor) NAOC/PMO, CAS

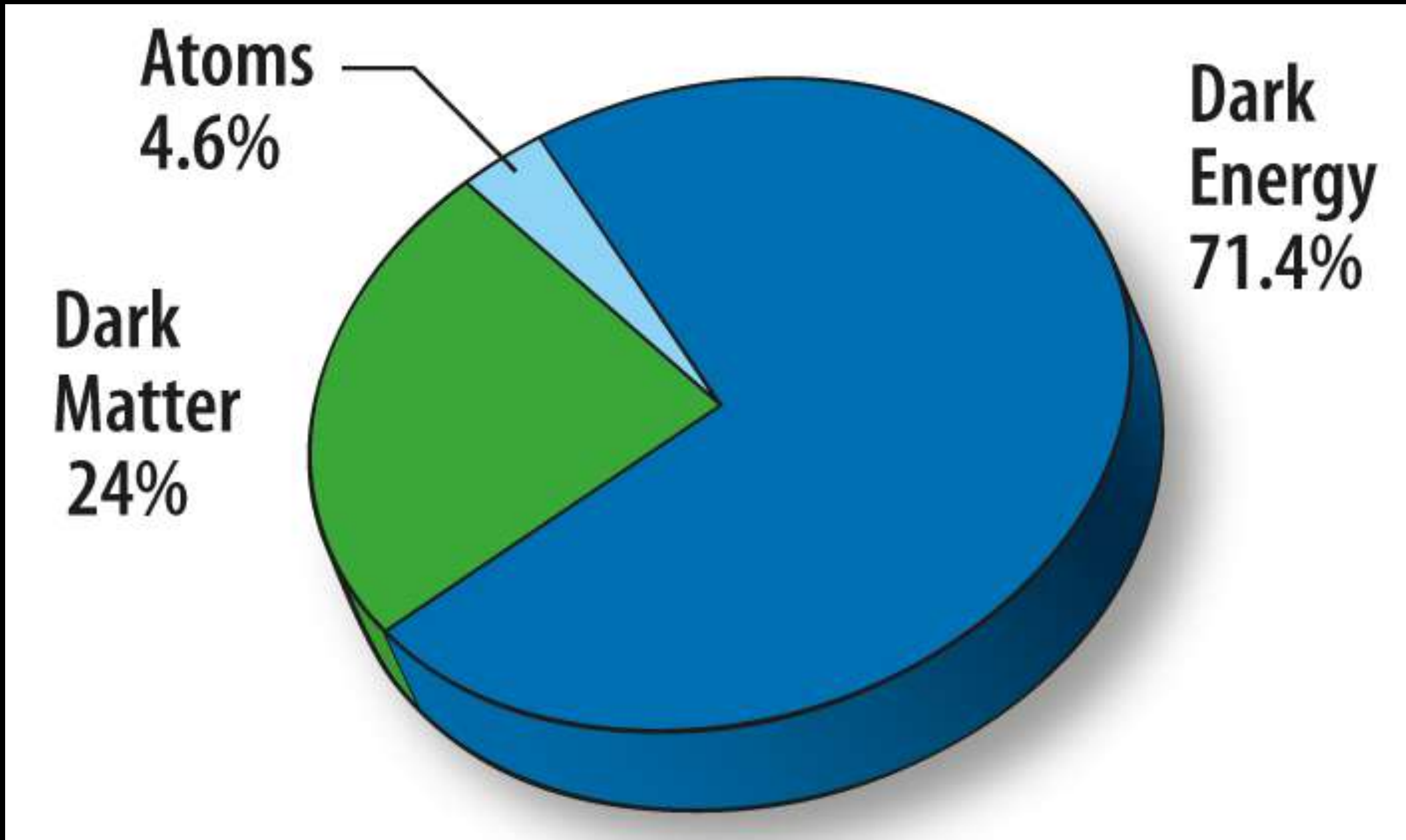

Collaborators: R. Battye, D. Contreras, C. Dickinson, C. Hernandez-Monteagudo, G. Hinshaw, A. Hojjati, Y.-C. Li, I. McCarthy, K. Moodley, M. Remazeilles, D. Scott, L. Staveley-Smith, H. Tanimura, D. Tramonte, L. Van Waerbeke, J. Zuntz, & Planck team

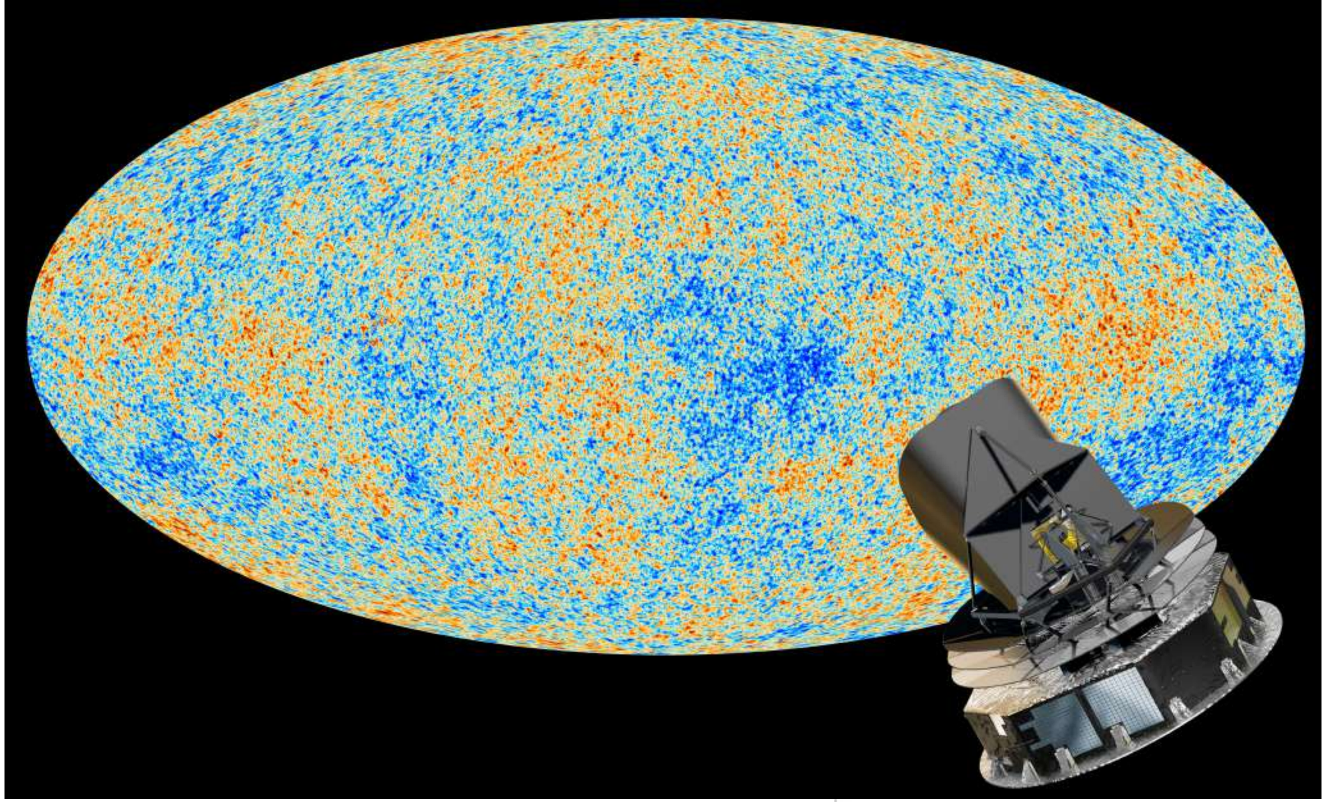

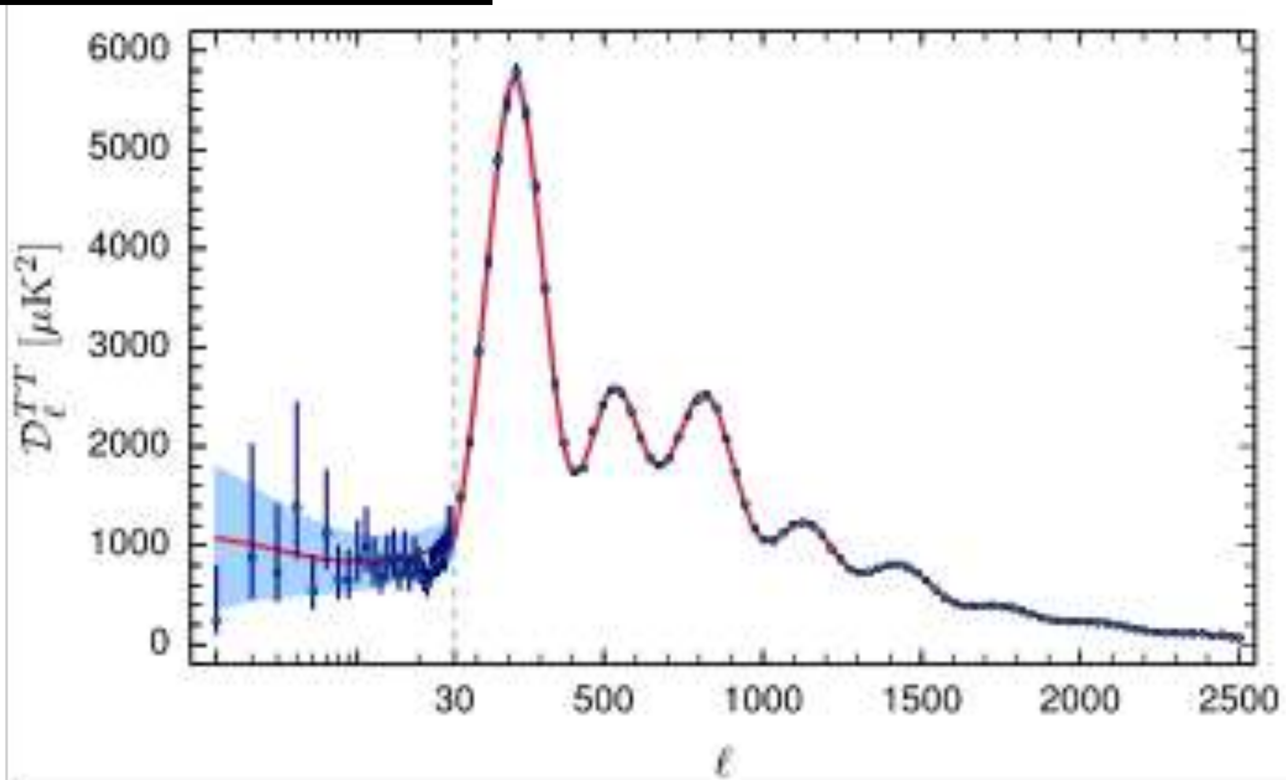

6000
5000
4000
3000
2000
1000
0
$\mathcal{D}_\ell^{TT}$ [μK^2]
30
500
1000
1500
2000
2500
ℓ

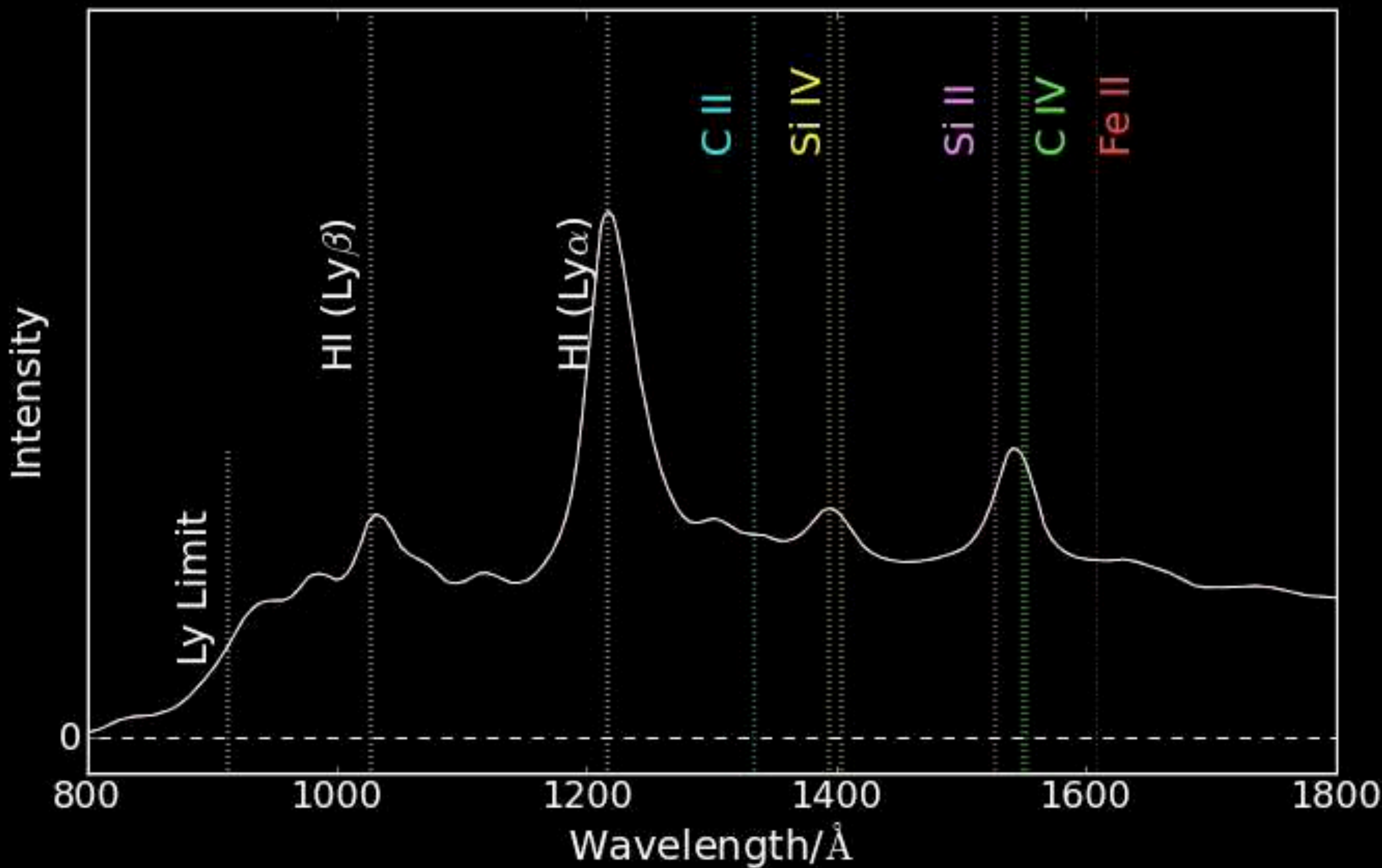
Intensity
Ly Limit
HI (Lyβ)
HI (Lyα)
C II
Si IV
Si II
C IV
Fe II
0
800
1000
1200
1400
1600
1800
Wavelength/Å

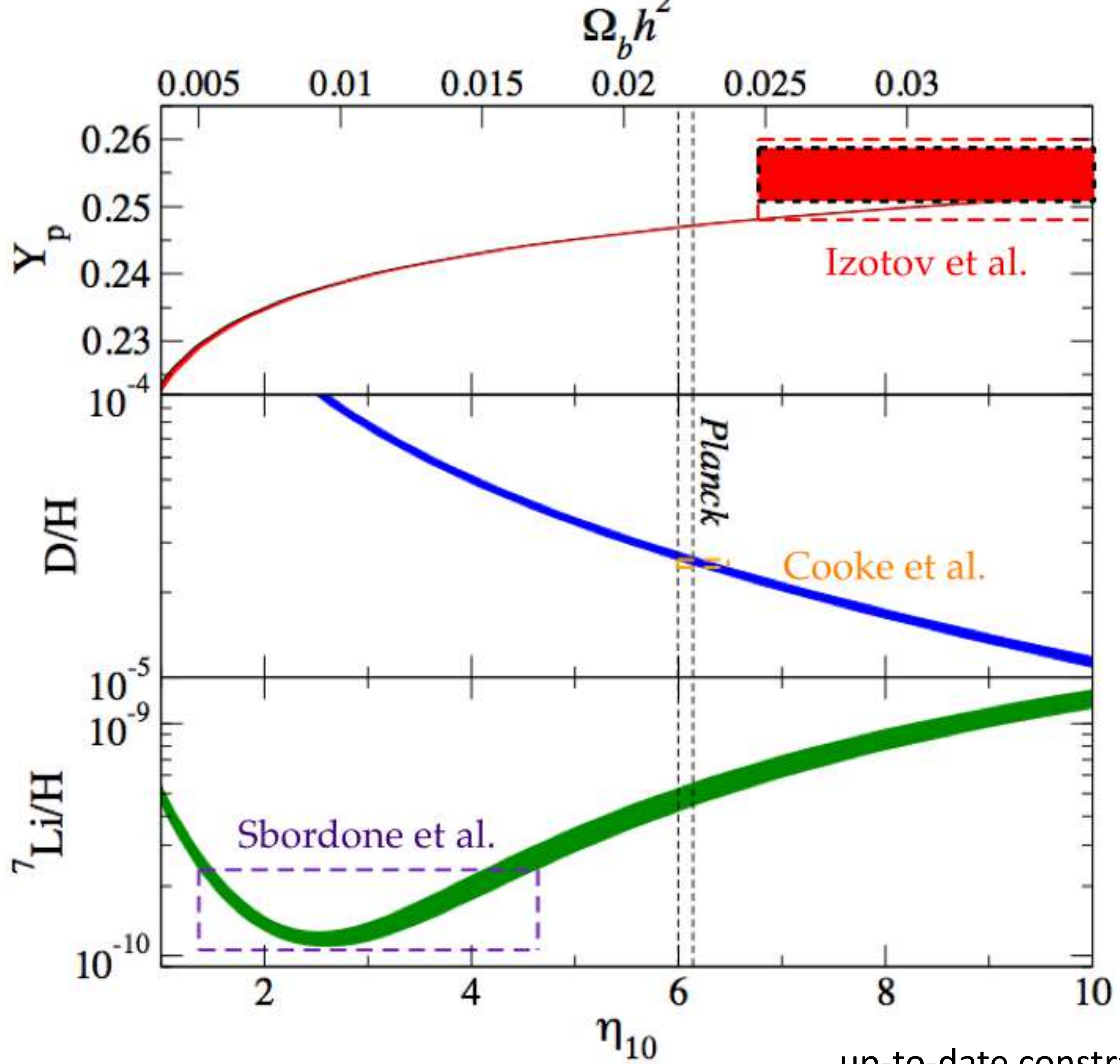

up-to-date constraints by 2019

$$100\Omega_b h^2(\text{BBN}) = 2.260 \pm 0.018 \pm 0.029$$

Cooke+ 2016

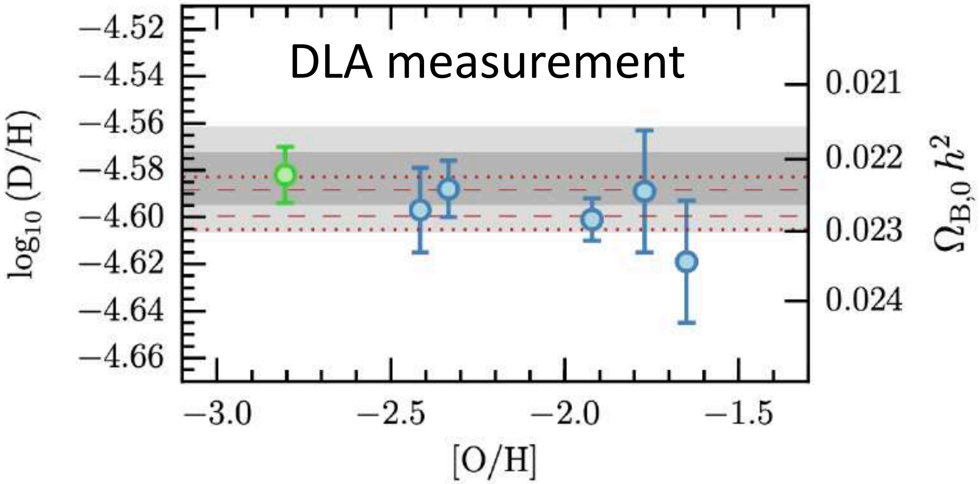

$$100\Omega_b h^2(\text{CMB}) = 2.226 \pm 0.023$$

Planck collaboration 2018 (including YZM)

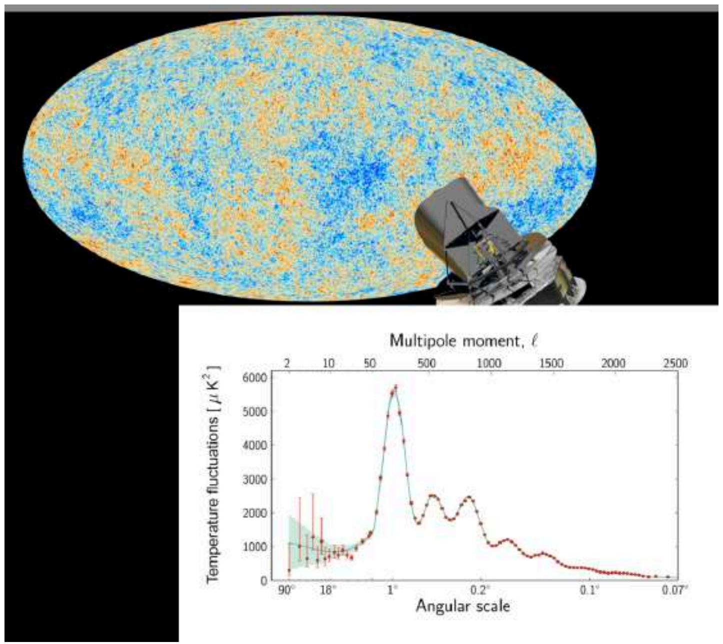

$$100\Omega_b h^2(\text{FRB}) = 2.405 \pm 1.085$$

Macquart et al. 2020, Nature

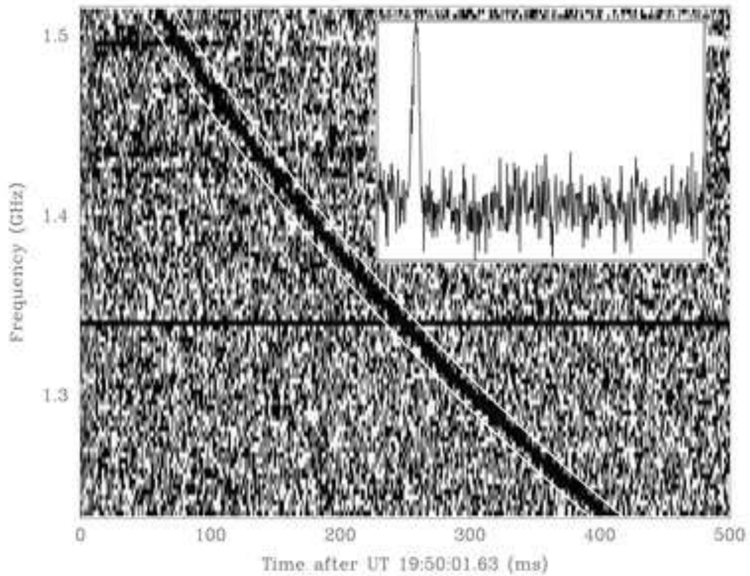

Contributions to DM

$$DM_{\mathrm{E}} \equiv DM_{\mathrm{obs}} - DM_{\mathrm{MW}} = DM_{\mathrm{IGM}} + DM_{\mathrm{HG}}$$

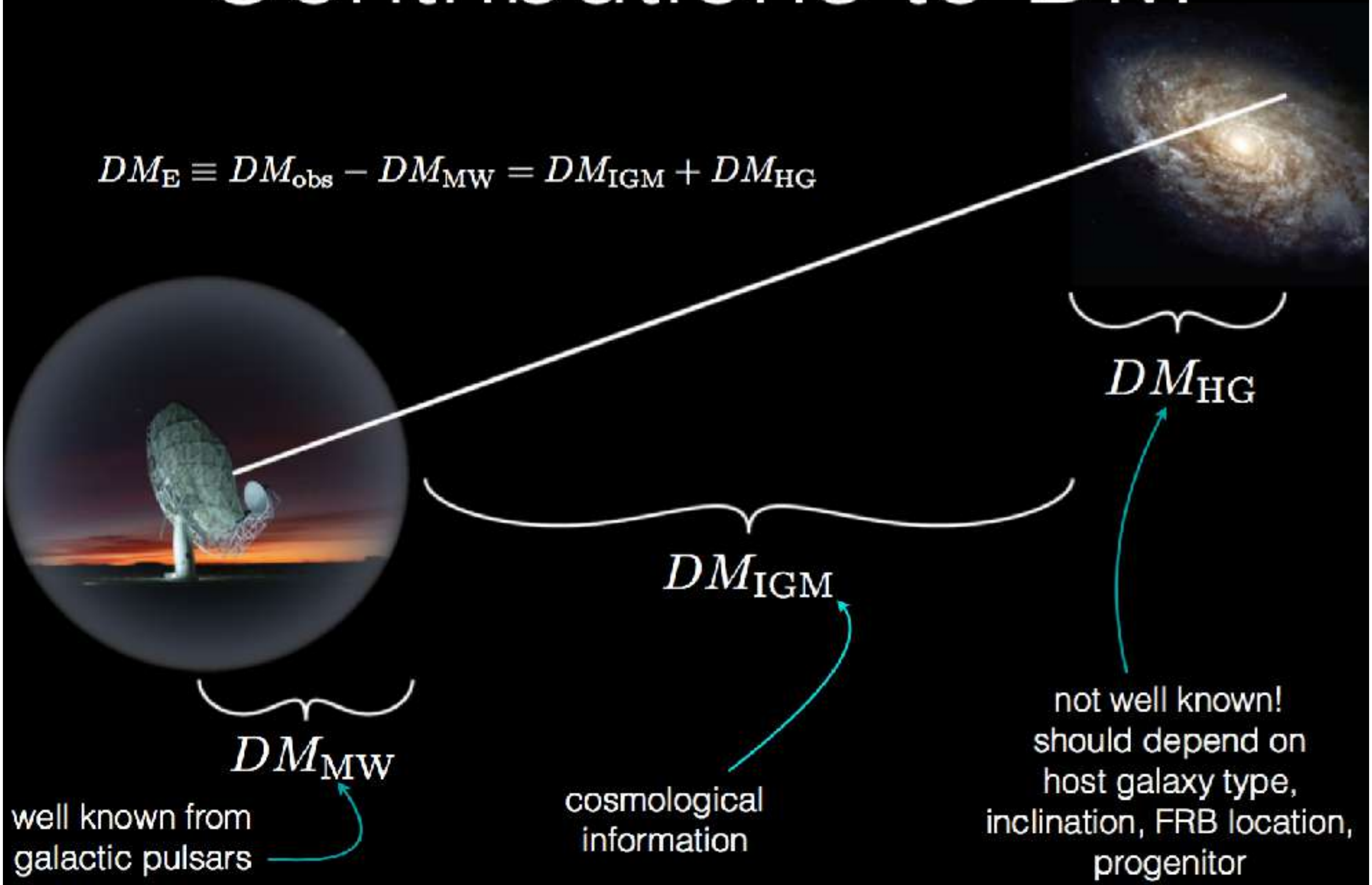

Model parameter

$100\Omega_b h^2(\mathrm{BBN}) = 2.260 \pm 0.018 \pm 0.029$

Cooke+ 2016

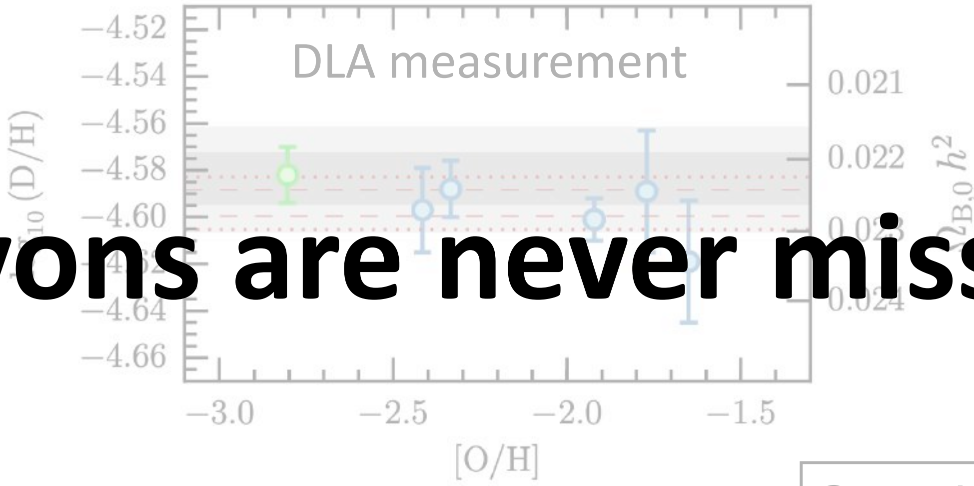

Baryons are never missing!

Counting from dispersion

We just haven’t counted enough of them at low redshifts

$100\Omega_b h^2(\mathrm{CMB}) = 2.2$[illegible]$6 \pm 0.015$

Planck collaboration 2018 (including YZM)

$100\Omega_b h^2(\mathrm{FRB}) = 2.$[illegible]$ \pm 1.085$

Macquart et al. 2020, Nature

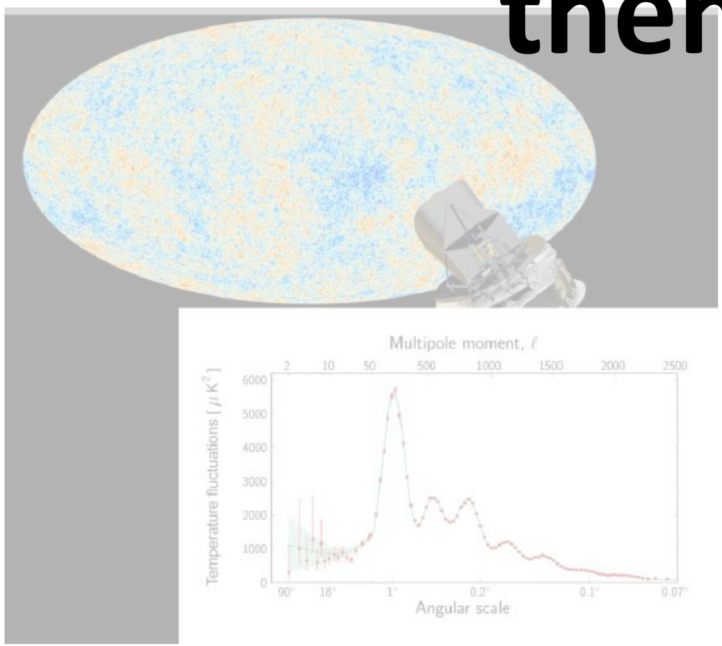

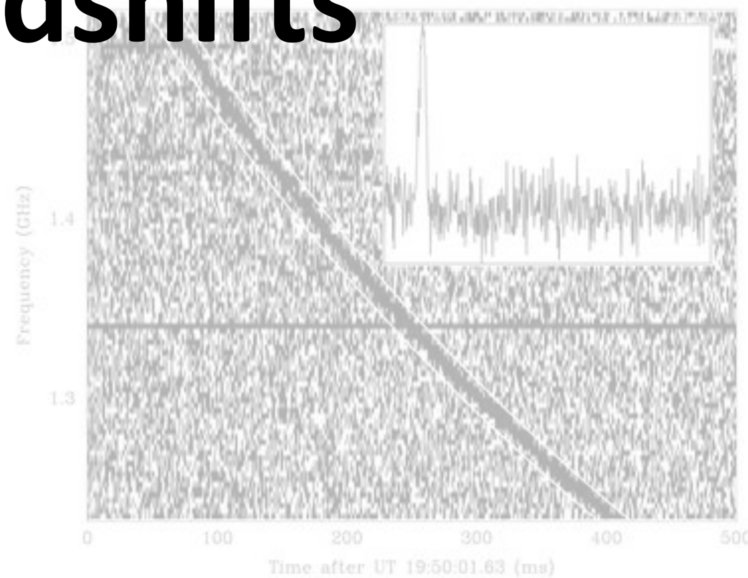

Cosmic baryon inventory:

Category	Parameter	Components[a]
3.3................................	Main-sequence stars: spheroids and bulges	0.0015 ± 0.0004
3.4................................	Main-sequence stars: disks and irregulars	0.00055 ± 0.00014
3.5................................	White dwarfs	0.00036 ± 0.00008
3.6................................	Neutron stars	0.00005 ± 0.00002
3.7................................	Black holes	0.00007 ± 0.00002
3.8................................	Substellar objects	0.00014 ± 0.00007
3.9................................	H I + He I	0.00062 ± 0.00010
3.10..............................	Molecular gas	0.00016 ± 0.00006
3.11..............................	Planets	10^{-6}
3.12..............................	Condensed matter	$10^{-5.6 \pm 0.3}$
3.13..............................	Sequestered in massive black holes	$10^{-5.4}(1 + \epsilon_n)$

3.3+…+3.13: $\Omega_{b,g} = 0.0035$ =8% total baryon density

90% of baryons are in either intergalactic or intercluster medium

Fukugita, & Peebles 2004

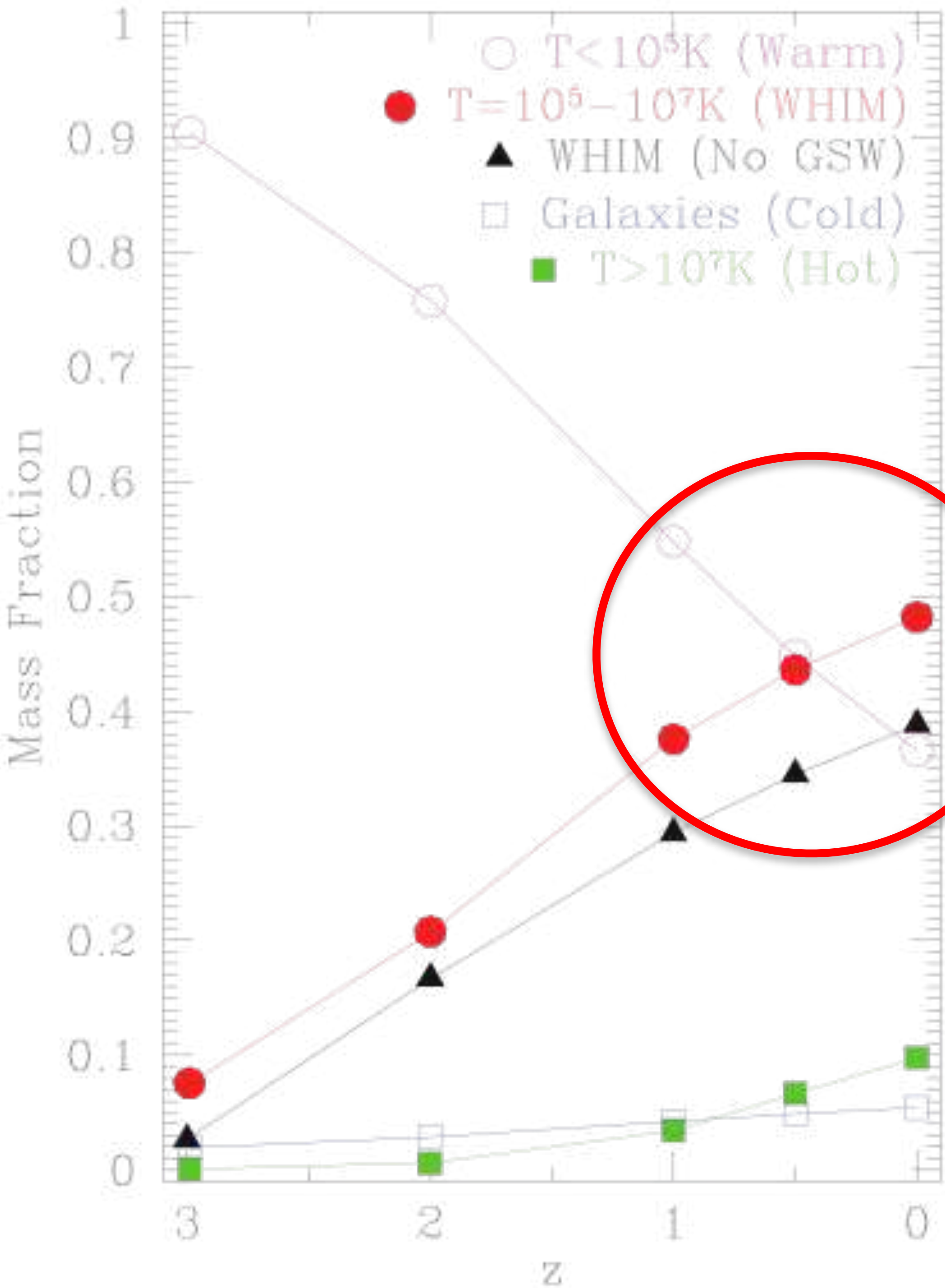

Cen and Ostriker 2006

X-ray: ~ $n_e^2(r)$

thermal Sunyaev-Zeldovich effect X Weak Lensing

__YZM__, L. Van Waerbeke et al., 2015, JCAP, 09, 046
A. Hojjati, I. McCarthy, J. Harnois-Deraps, __YZM__ et al., 2015, JCAP, 10, 047
A. Hojjati, …. , __YZM__,… 2017, JCAP, 471, 1565

Thermal SZ maps X Luminous red galaxies

H Tanimura, …, __YZM__,… et al. 2018, MNRAS, 483, 223

kinetic Sunyaev-Zeldovich effect X Peculiar velocity field

Planck intermediate results XXXVII, 2016, A&A, 586, 140
C.Hernandez-Monteagudo, __YZM__, F-S Kitaura, W.Wang et al., 2015, Phys. Rev. Lett. 115, 191301
Yi-Chao Li, __YZM__, Mathieu Remazeilles, Kavilan Moodley, 2018, PRD, 97, 023514

kinetic SZ effect X MCXC clusters

Planck intermediate results LIII, 2018, A&A, 617, A48

The Observation of Relic Radiation as a Test of the Nature of X-Ray Radiation from the Clusters of Galaxies

1972

Mon. Not. R. astr. Soc. (1980) 190, 413–420

The velocity of clusters of galaxies relative to the microwave background. The possibility of its measurement

R. A. Sunyaev and Ya. B. Zeldovich *Academy of Sciences, USSR, Space Research Institute, Profsoyuznaja 88, 117810 Moscow, USSR*

Received 1979 May 31

1980

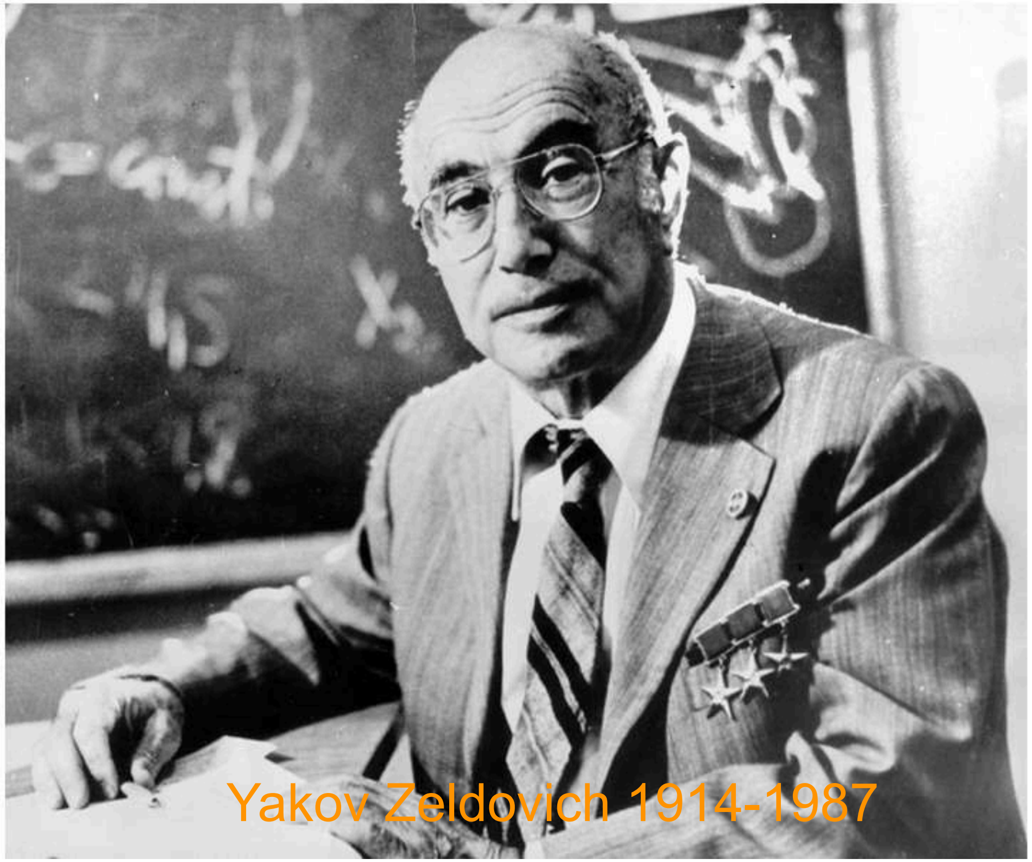

thermal Sunyaev-Zeldovich effect X **Weak Lensing**

__YZM__, L. Van Waerbeke et al., 2015, JCAP, 09, 046
A. Hojjati, I. McCarthy, J. Harnois-Deraps, __YZM__ et al., 2015, JCAP, 10, 047
A. Hojjati, …. , __YZM__,… 2017, JCAP, 471, 1565

Thermal SZ maps X Luminous red galaxies

H Tanimura, …, __YZM__,… et al. 2018, MNRAS, 483, 223

—>HI (21-cm) intensity mapping X Central galaxies

D. Tramonte, __YZM__, Y.C. Li, L. Staveley-Smith, 2019, MNRAS

kinetic Sunyaev-Zeldovich effect X Peculiar velocity field

Planck intermediate results XXXVII, 2016, A&A, 586, 140
C.Hernandez-Monteagudo, __YZM__, F-S Kitaura, W.Wang et al., 2015, Phys. Rev. Lett. 115, 191301
Yi-Chao Li, __YZM__, Mathieu Remazeilles, Kavilan Moodley, 2018, PRD, 97, 023514

kinetic SZ effect X MCXC clusters

Planck intermediate results LIII, 2018, A&A, 617, A48

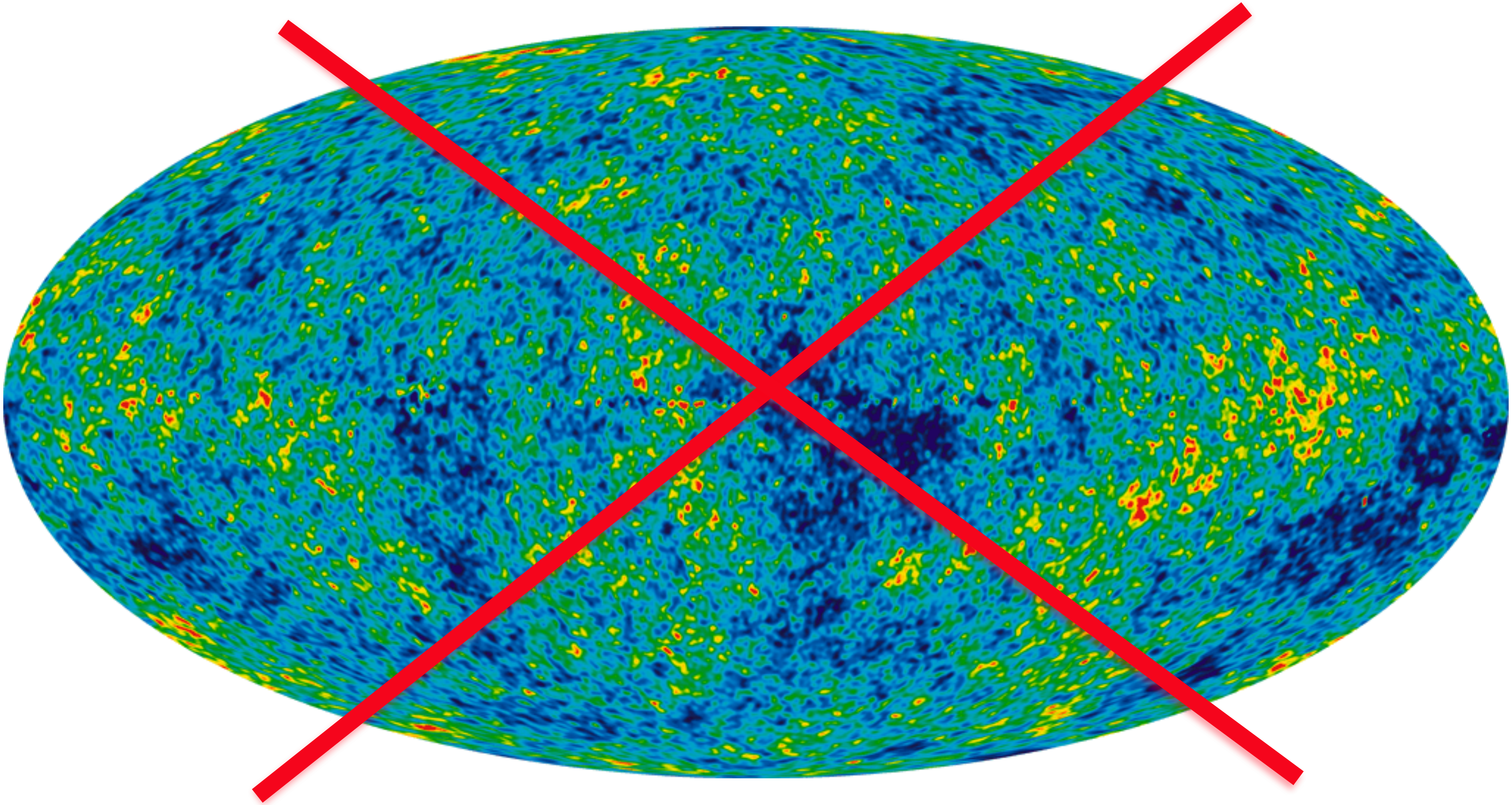

The thermal Sunyaev-Zeldovich effect

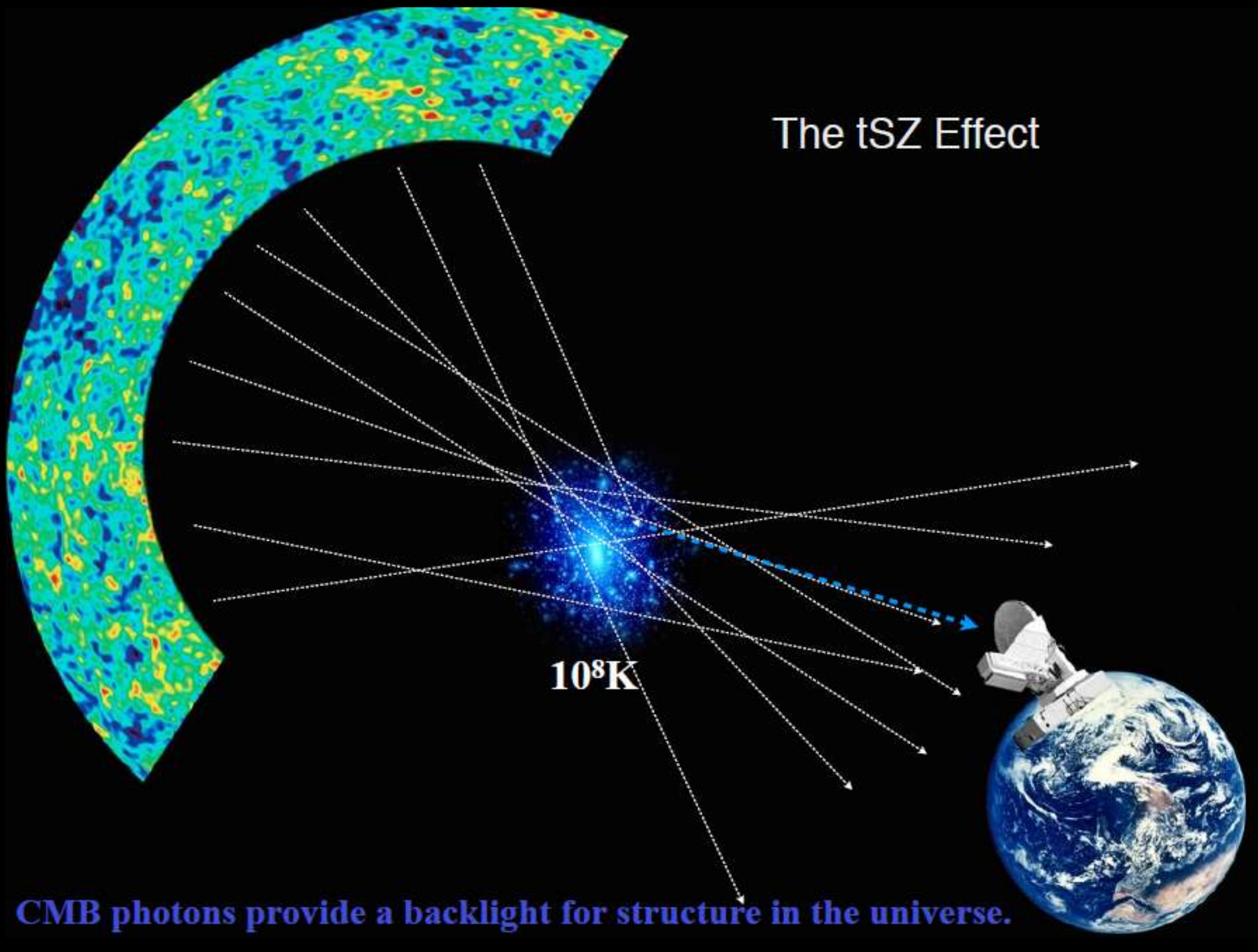

Thermal Sunyaev-Zeldovich effect (tSZ):

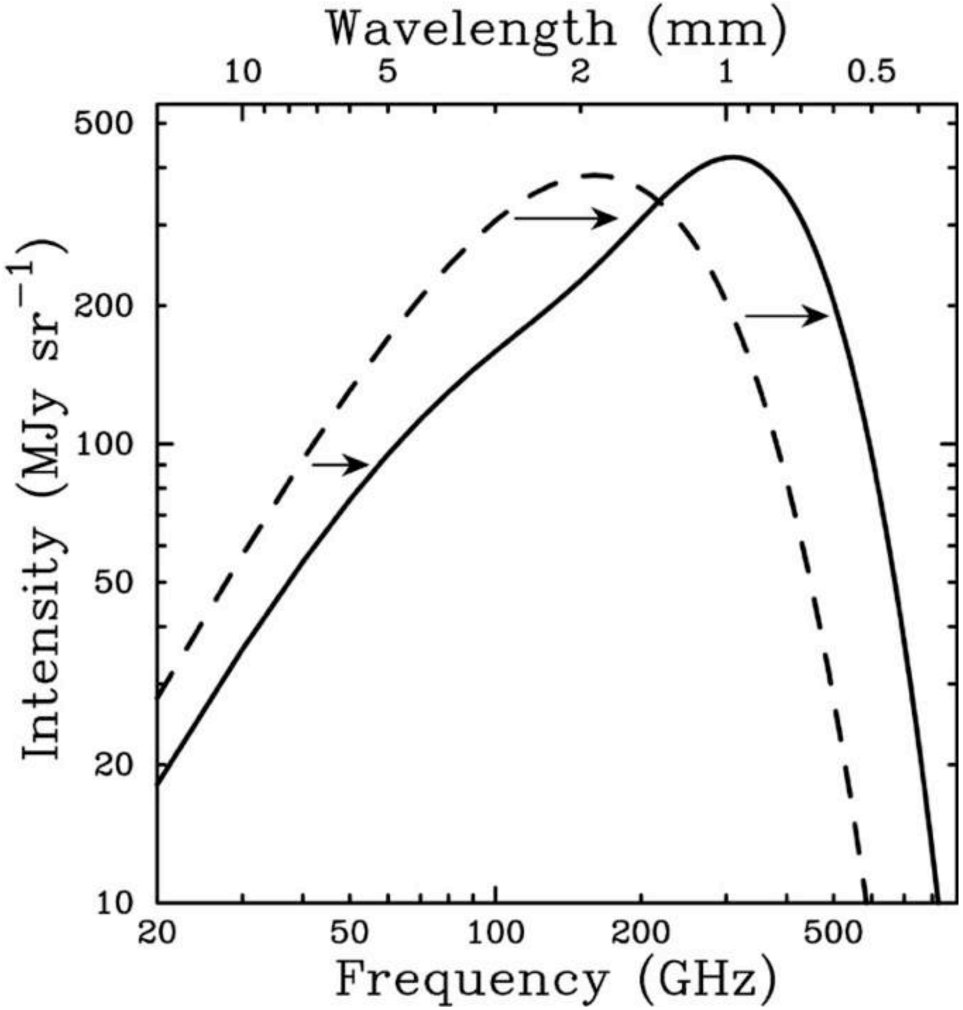

$$\frac{\Delta T}{T} = \left[\eta \frac{e^{\eta}+1}{e^{\eta}-1} - 4\right] y \equiv g_{\nu} y$$

$$g_{\nu} \equiv (\eta(e^{\eta}+1)/(e^{\eta}-1))-4$$

$$\eta = \frac{h\nu}{k_B T_{\mathrm{CMB}}} = \frac{h\nu_0}{k_B T_0} = 1.76\left(\frac{\nu_0}{100\mathrm{GHz}}\right)$$

$$y = \frac{k_B \sigma_T}{m_e c^2} \int_0^l T_e(l) n_e(l)\, \mathrm{d}l$$

WMAP:

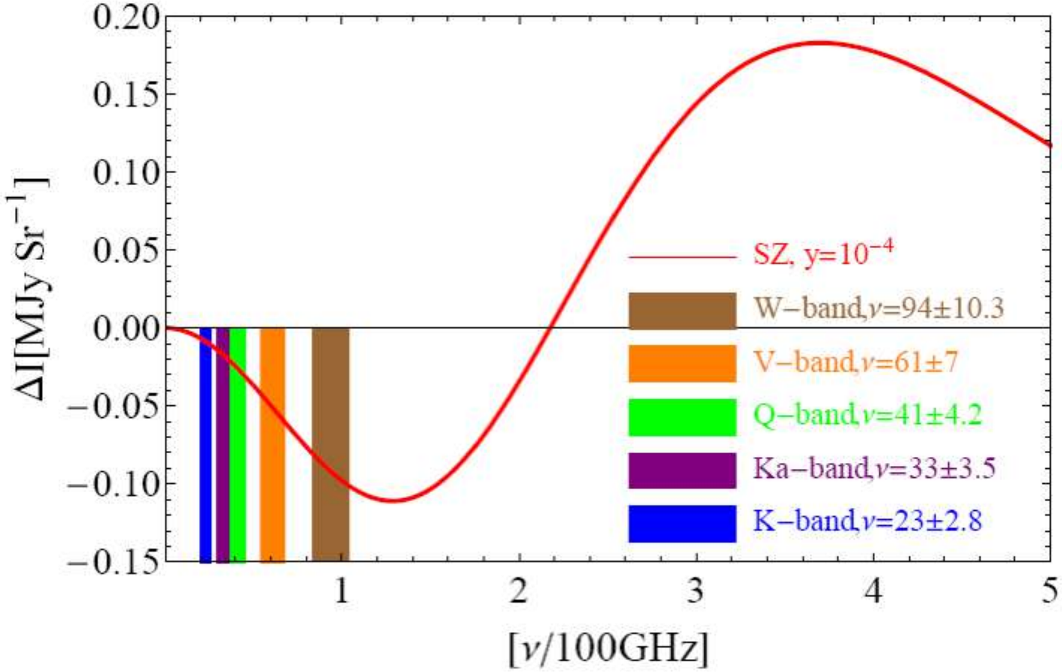

0.20
0.15
0.10
0.05
0.00
−0.05
−0.10
−0.15
1
2
3
4
5
ΔI[MJy Sr^{-1}]
[ν/100GHz]
SZ, y=10^{-4}
W−band,ν=94±10.3
V−band,ν=61±7
Q−band,ν=41±4.2
Ka−band,ν=33±3.5
K−band,ν=23±2.8

Planck:

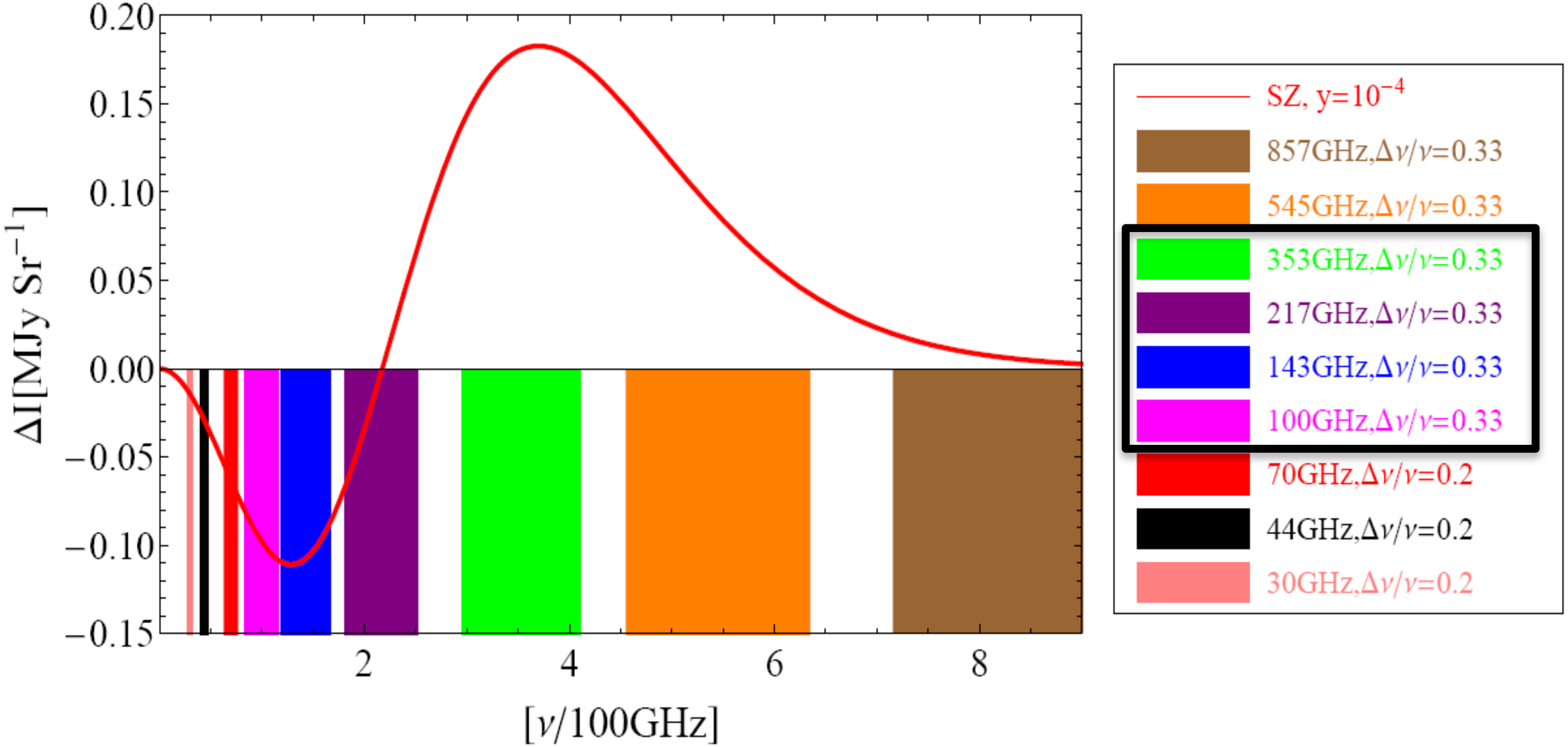

0.20
0.15
0.10
0.05
0.00
−0.05
−0.10
−0.15
2
4
6
8
ΔI[MJy Sr^{-1}]
[ν/100GHz]
SZ, y=10^{-4}
857GHz,Δν/ν=0.33
545GHz,Δν/ν=0.33
353GHz,Δν/ν=0.33
217GHz,Δν/ν=0.33
143GHz,Δν/ν=0.33
100GHz,Δν/ν=0.33
70GHz,Δν/ν=0.2
44GHz,Δν/ν=0.2
30GHz,Δν/ν=0.2

Planck SZ y map, version E

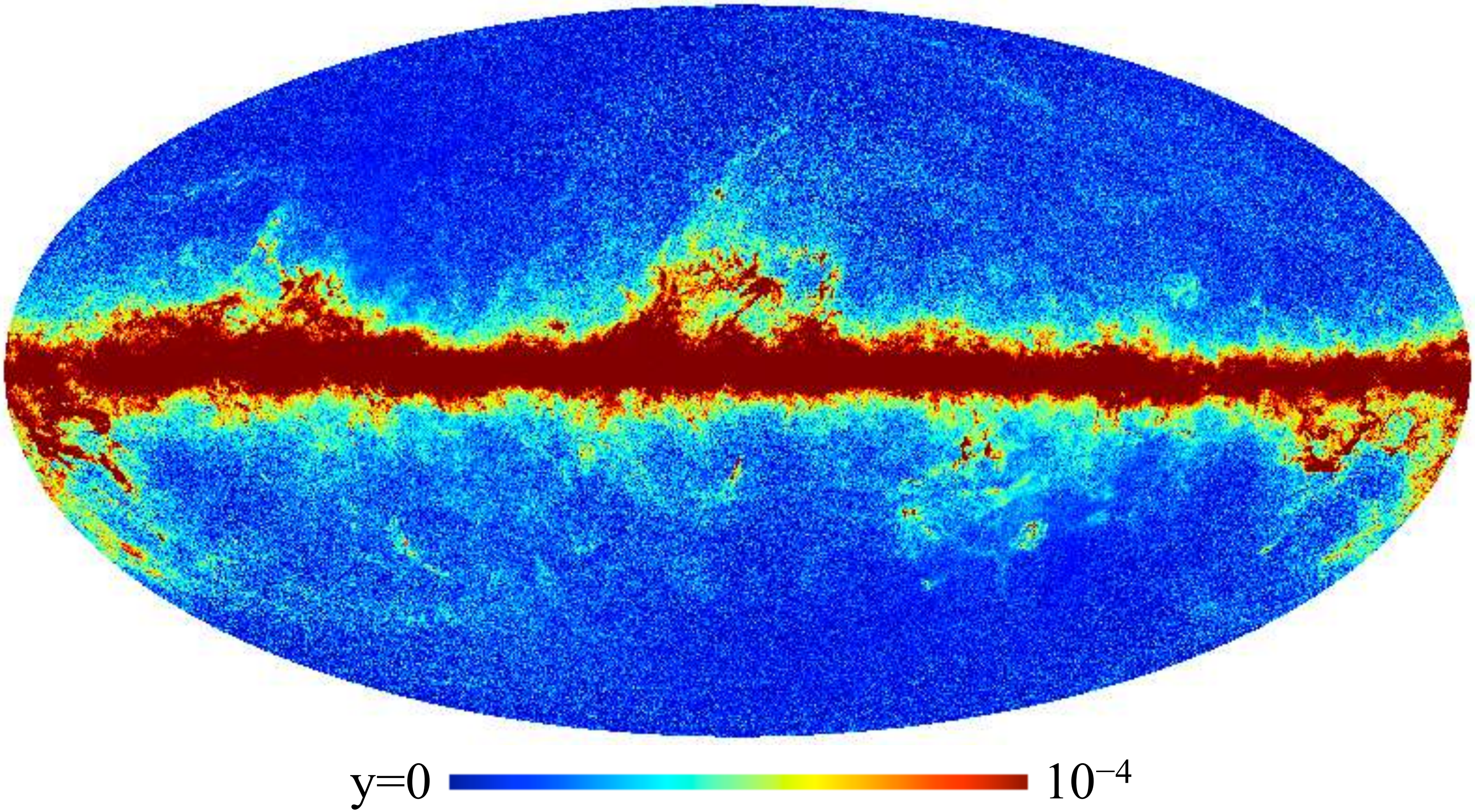

Reject $\beta_{dust} = 2.0$, $r_{2.0}(100\ \mathrm{GHz}) = 0$

CFHT mass map:

154 deg^2 in 4 patches

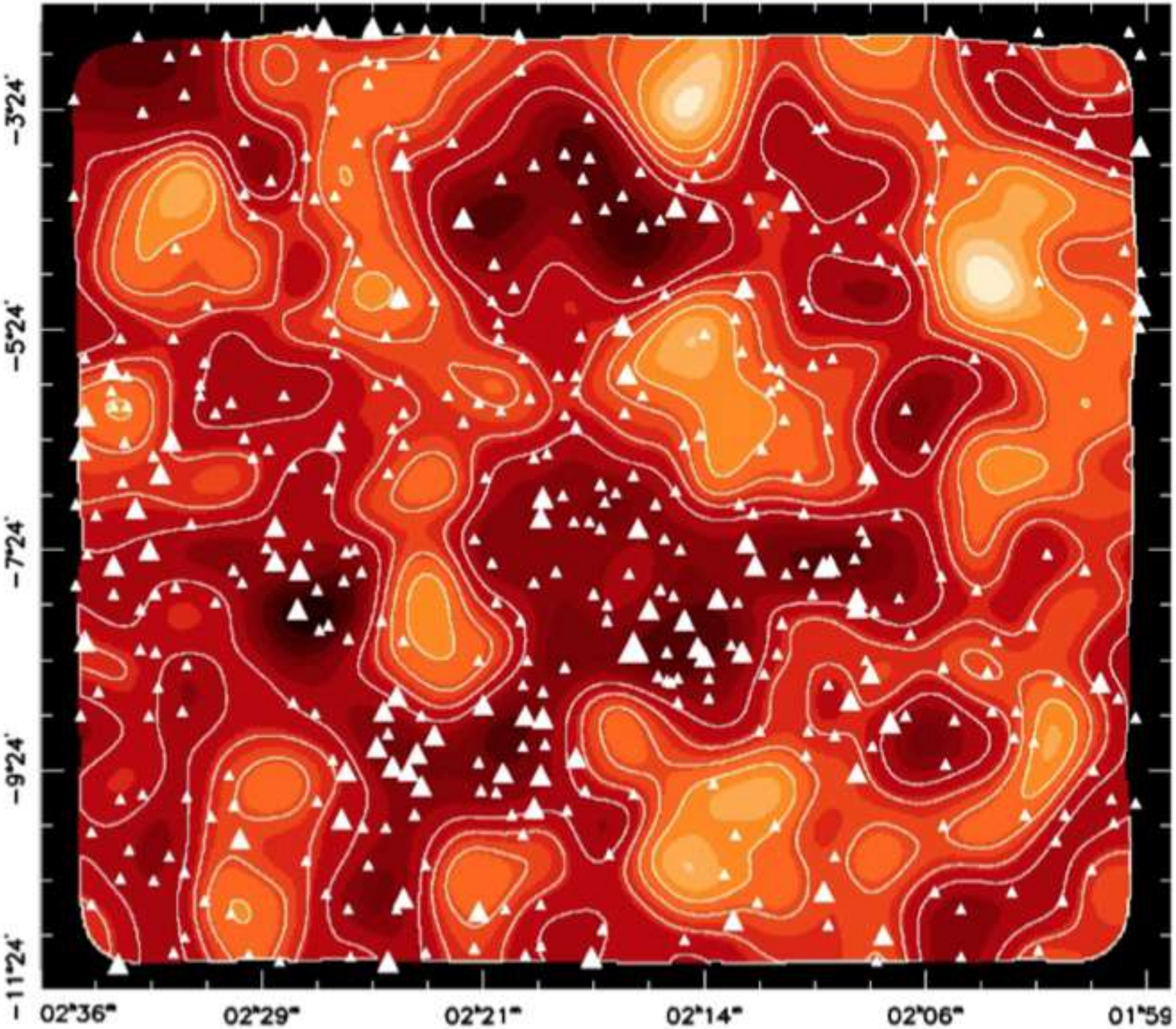

Van Waerbeke et al., 2014, MNRAS

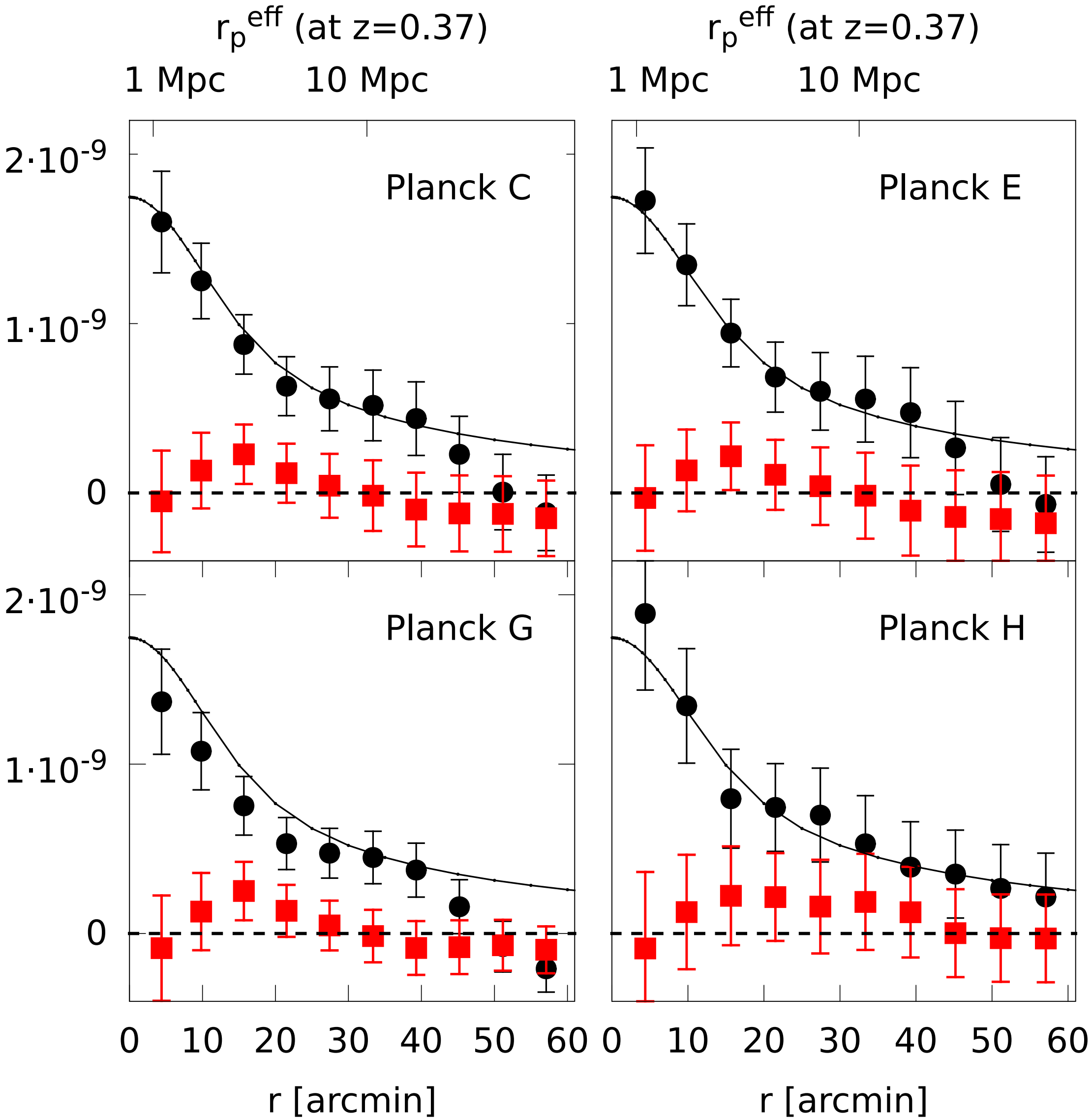

Red squares are for cross-correlation with lensing B-mode

van Waerbake, Hinshaw, Murray: 2014 Phys. Rev. D

Halo model:

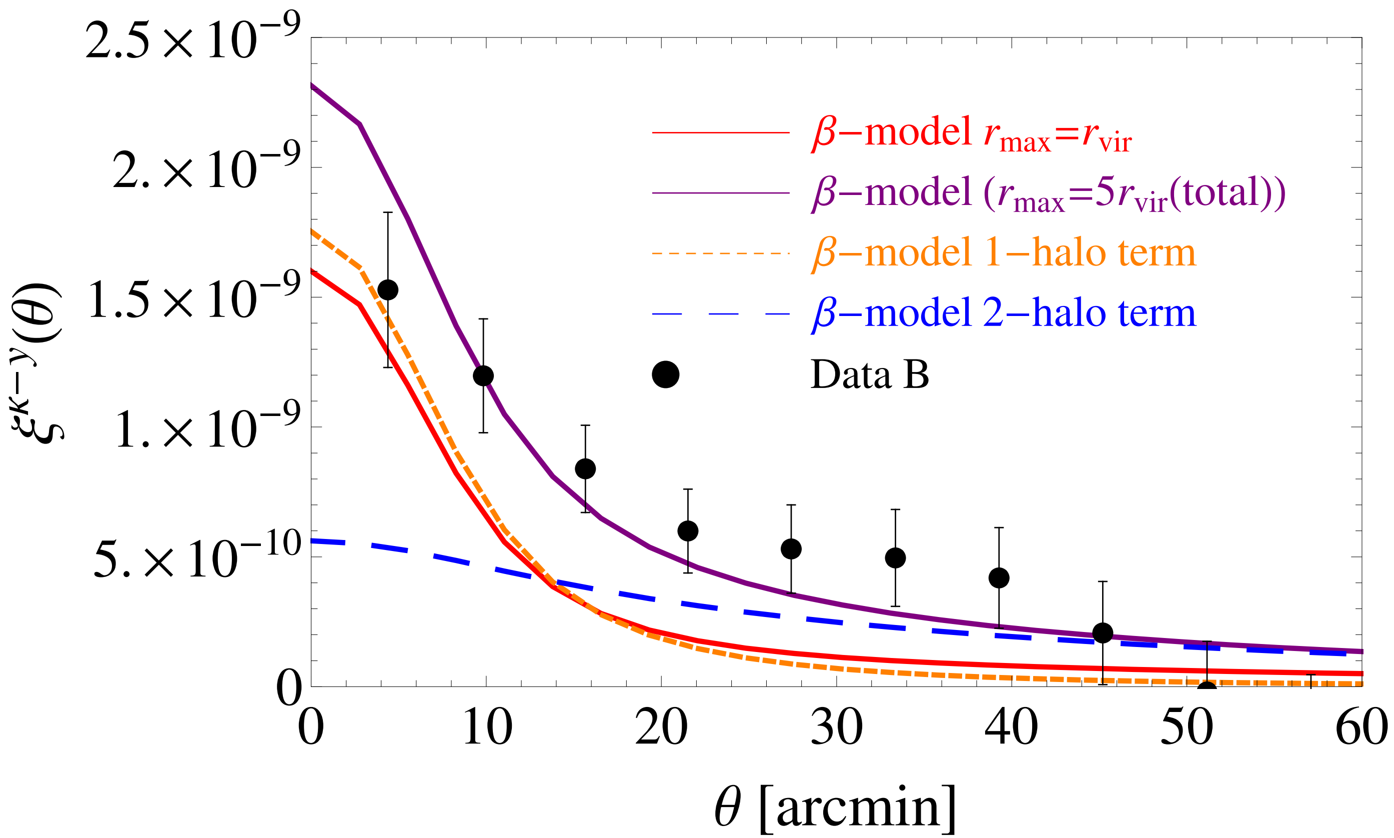

Ma et al. fits a halo model to the observed correlation function. A β model fits well, but in this context the data requires a 2-halo term to fit the large angular scale separation.

YZM, L. Van Waerbeke et al., 2015, JCAP, 09, 046
A. Hojjati, I. McCarthy, J. Harnois-Deraps, **YZM** et al., 2015, JCAP, 10, 047

	$10^{12}\,\mathrm{M}_\odot$–$10^{14}\,\mathrm{M}_\odot$	$10^{14}\,\mathrm{M}_\odot$–$10^{16}\,\mathrm{M}_\odot$
$(0.01\text{–}1)\,r_{\mathrm{vir}}$	26%	28%
$(1\text{–}100)\,r_{\mathrm{vir}}$	14%	32%

Virial theorem with $z = 0.37$, $M = 10^{12} - 10^{16}\mathrm{M}_\odot$

↓

$$T_\mathrm{e} = 10^5 - 10^7\,\mathrm{K}$$

YZM, L. Van Waerbeke et al., 2015, JCAP, 09, 046

A. Hojjati, I. McCarthy, J. Harnois-Deraps, **YZM** et al., 2015, JCAP, 10, 047

Red Cluster Sequence Lensing Survey (RCSLenS) X Planck thermal SZ effect map

Sky coverage: 560 deg^2   8.4 sigma detection

*A. Hojjati, …. , **YZM**,… 2017, JCAP, 471, 1565*

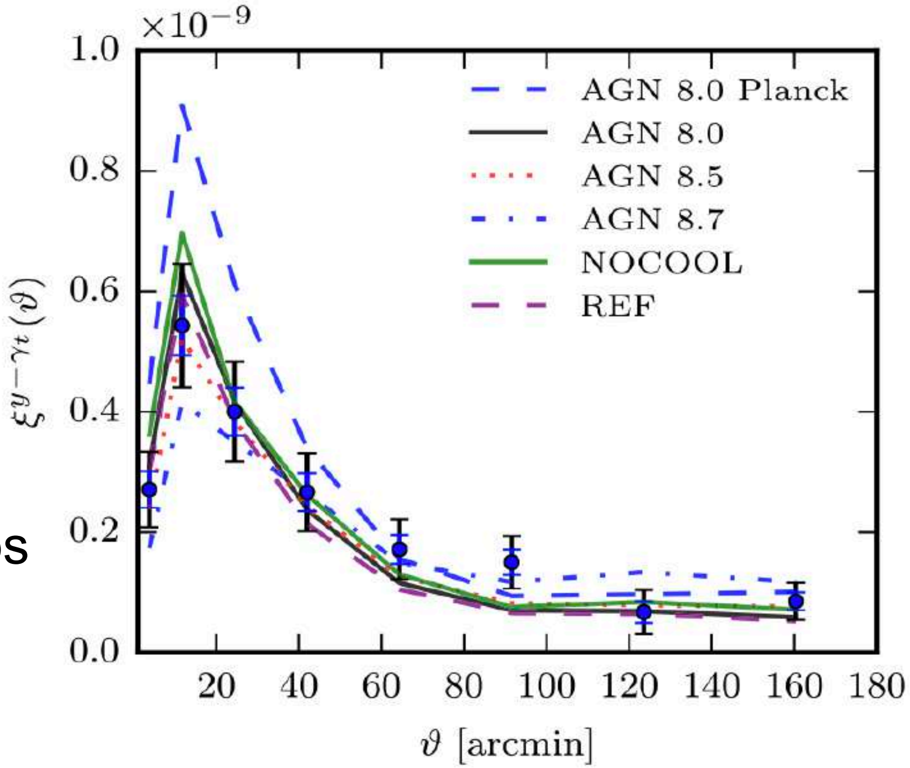

Recent works:

(1) DES Y3 lensing data X Planck+ACT maps — 21σ C.L.

Gatti, et al., arXiv: 2108.01600

Pandey, et al., arXiv: 2108.01601

(2) KiDS X Planck+ACT SZ maps —9σ C.L

Troster et al., arXiv: 2109.04458

thermal Sunyaev-Zeldovich effect X Weak Lensing

__YZM__, L. Van Waerbeke et al., 2015, JCAP, 09, 046
A. Hojjati, I. McCarthy, J. Harnois-Deraps, __YZM__ et al., 2015, JCAP, 10, 047
A. Hojjati, …. , __YZM__,… 2017, JCAP, 471, 1565

Thermal SZ maps X **Luminous red galaxies**

H Tanimura, …, __YZM__,… et al. 2018, MNRAS, 483, 223

kinetic Sunyaev-Zeldovich effect X Peculiar velocity field

Planck intermediate results XXXVII, 2016, A&A, 586, 140
C.Hernandez-Monteagudo, __YZM__, F-S Kitaura, W.Wang et al., 2015, Phys. Rev. Lett. 115, 191301
Yi-Chao Li, __YZM__, Mathieu Remazeilles, Kavilan Moodley, 2018, PRD, 97, 023514

kinetic SZ effect X MCXC clusters

Planck intermediate results LIII, 2018, A&A, 617, A48

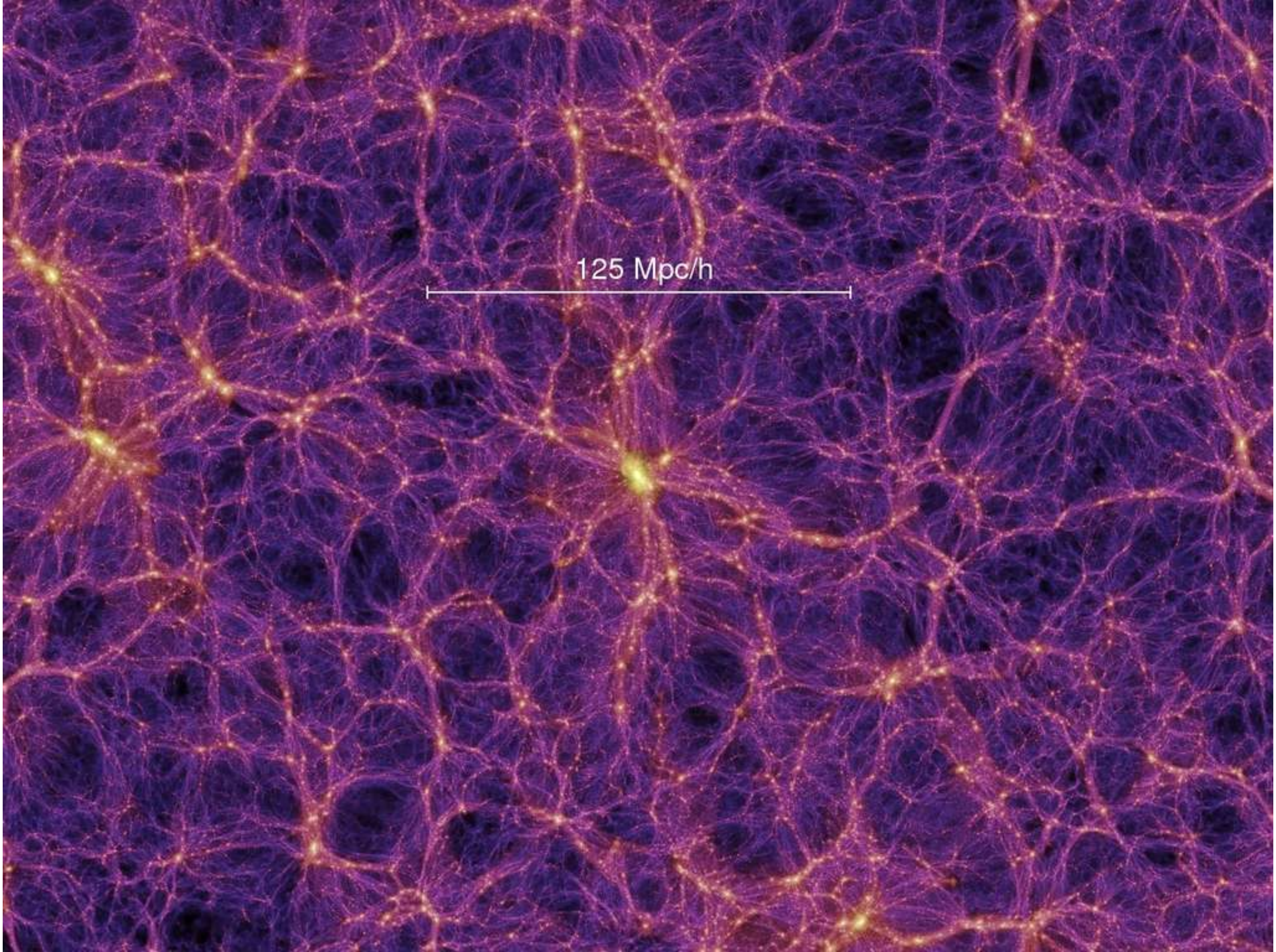
125 Mpc/h

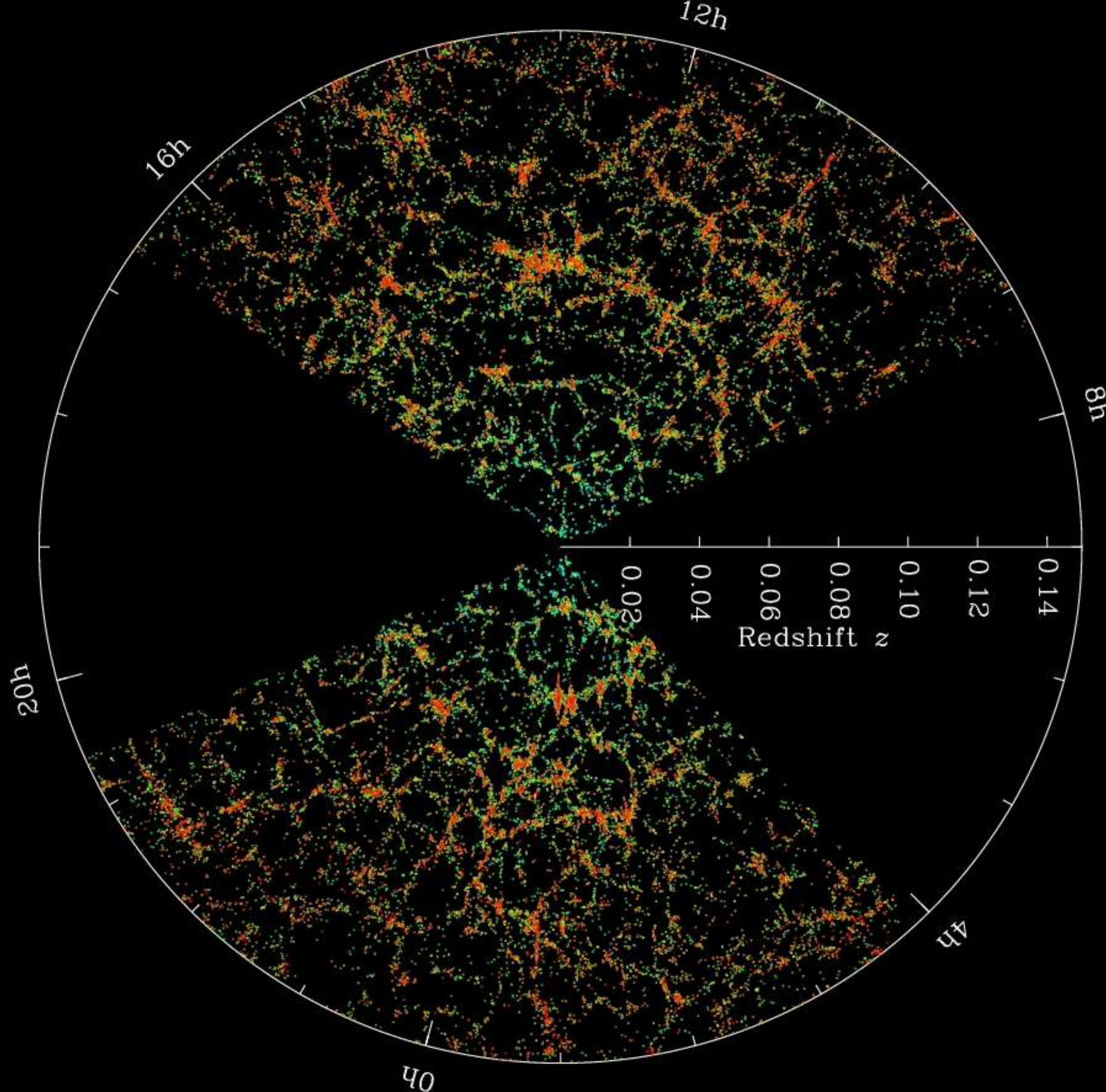
12h
16h
8h
20h
4h
0h
0.02
0.04
0.06
0.08
0.10
0.12
0.14
Redshift z

Stacking LRG/SDSS pairs (Ms>11.3, 0.15<z<0.43 (N=28247)) on Planck y-map

tangential distance: 6-10 h^{-1}Mpc

radial distance: $\pm$ 6 h^{-1}Mpc

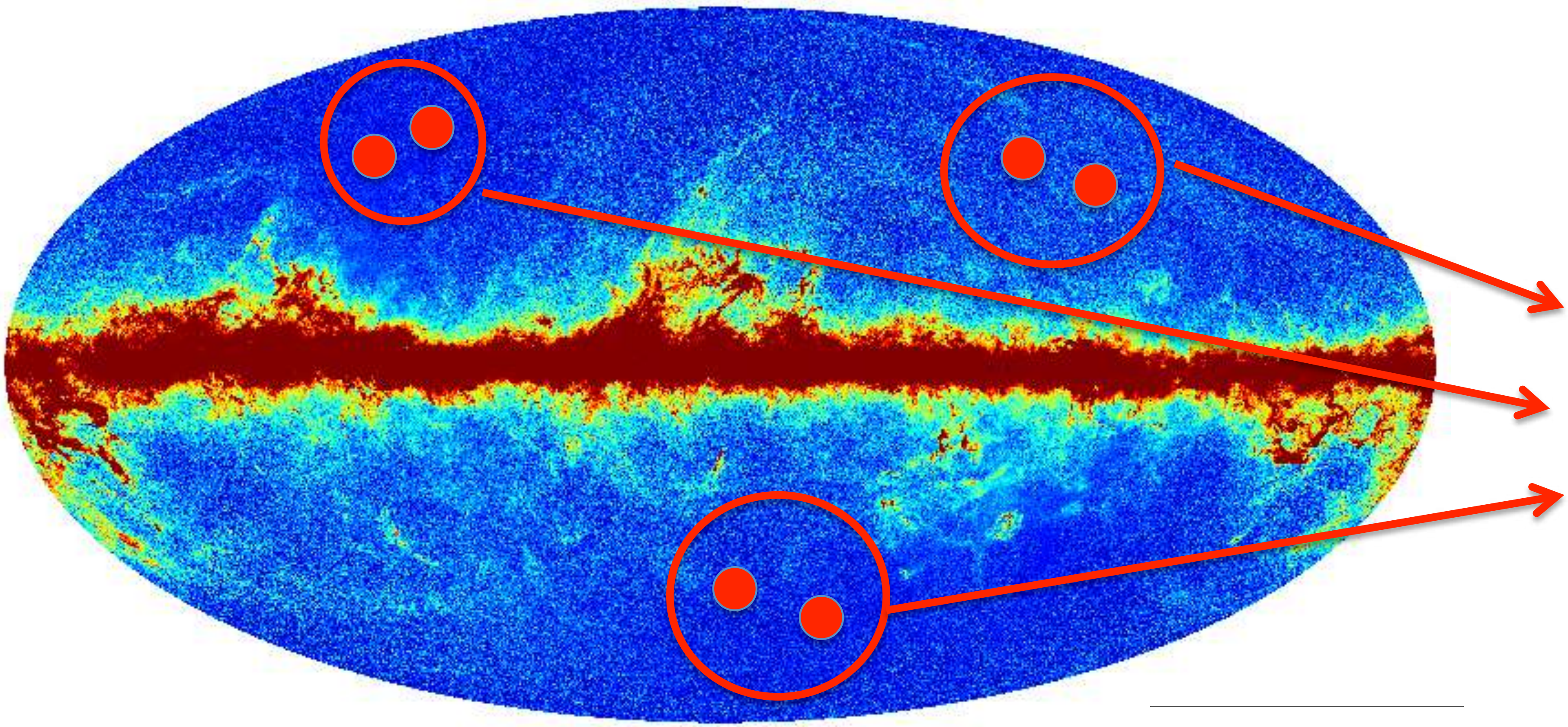

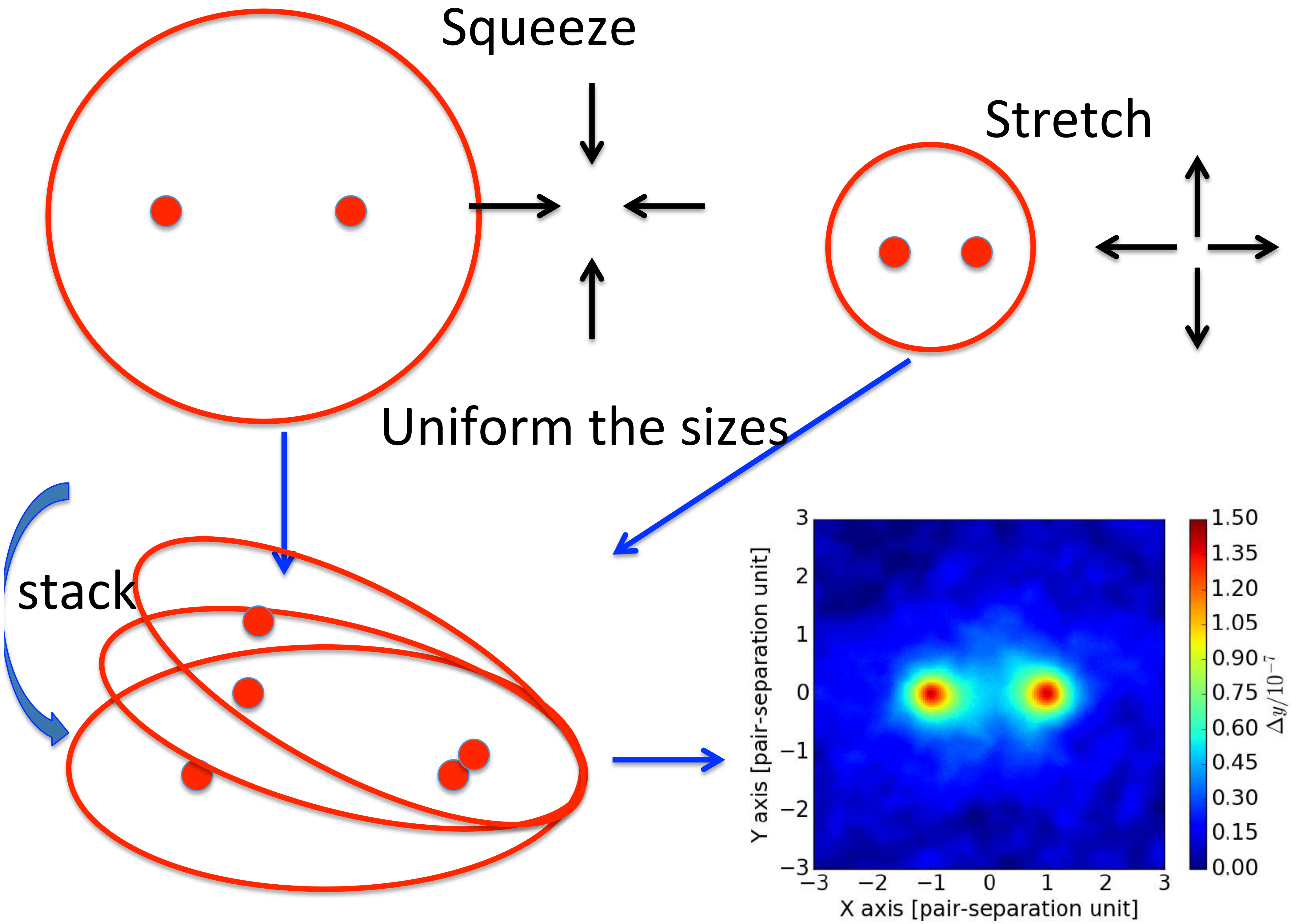

Squeeze
Stretch
Uniform the sizes
stack
Y axis [pair-separation unit]
X axis [pair-separation unit]
$\Delta y/10^{-7}$

Stacked

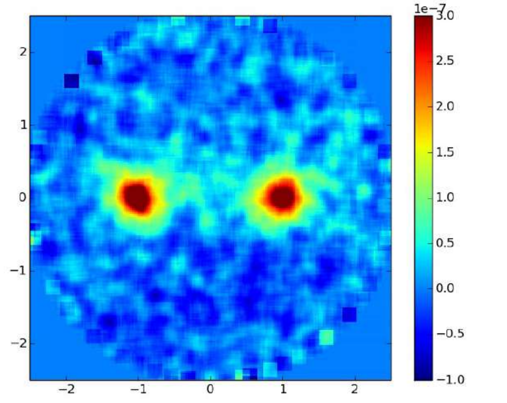

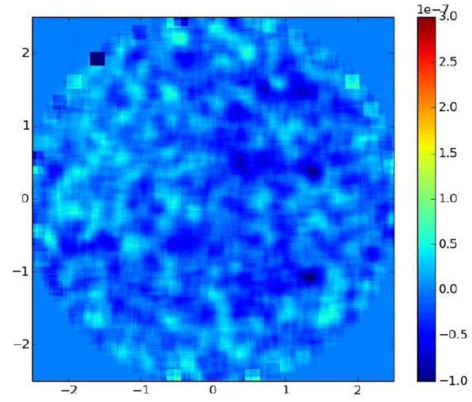

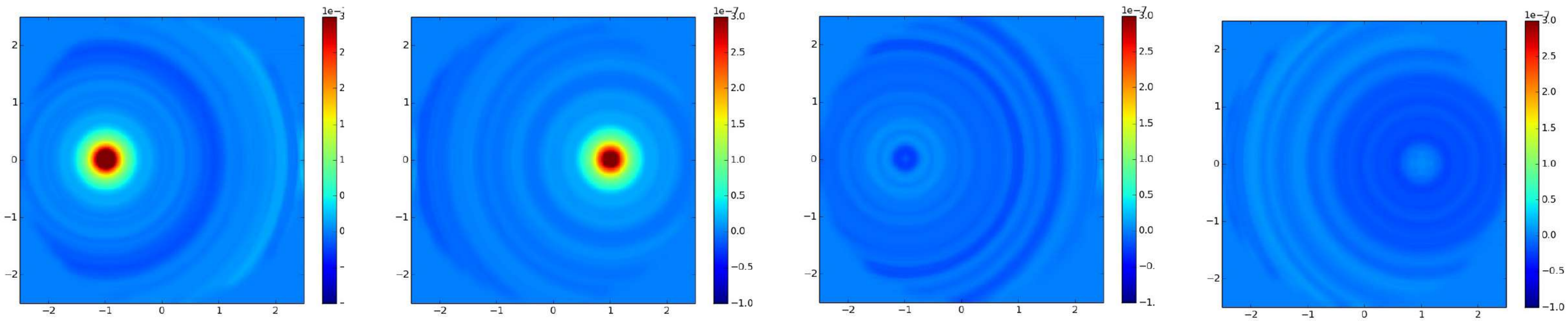

LRG SZ
Subtracted

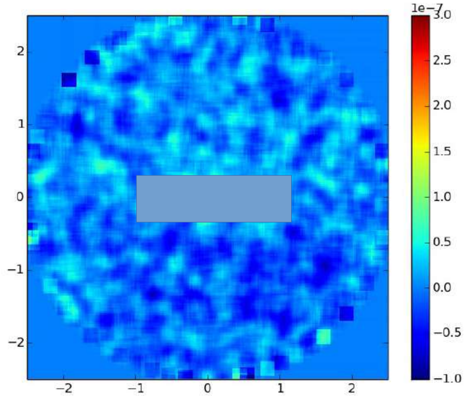

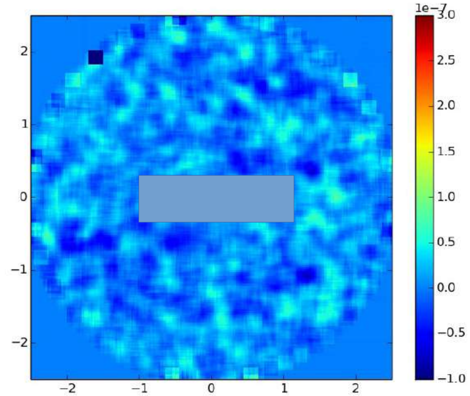

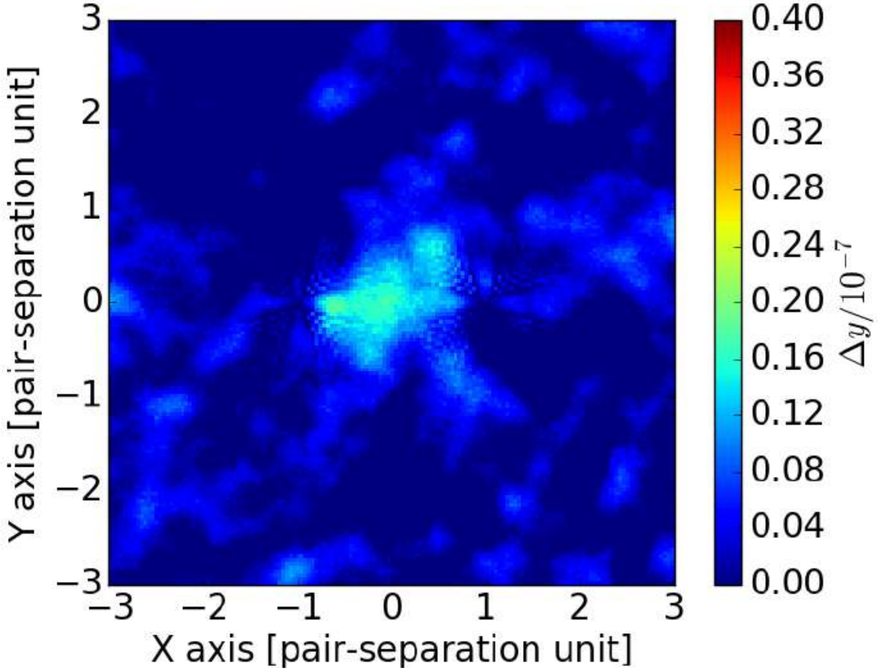

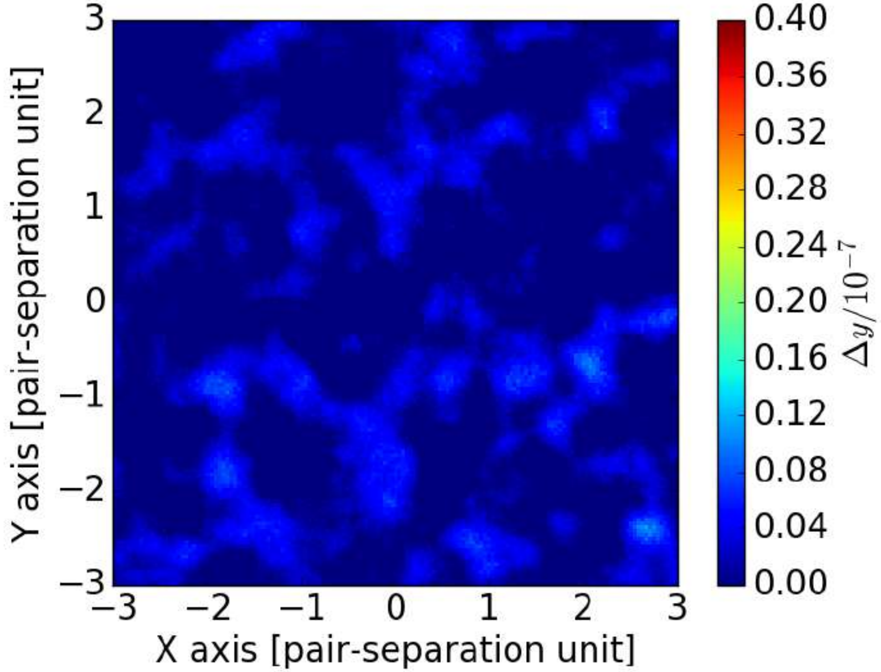

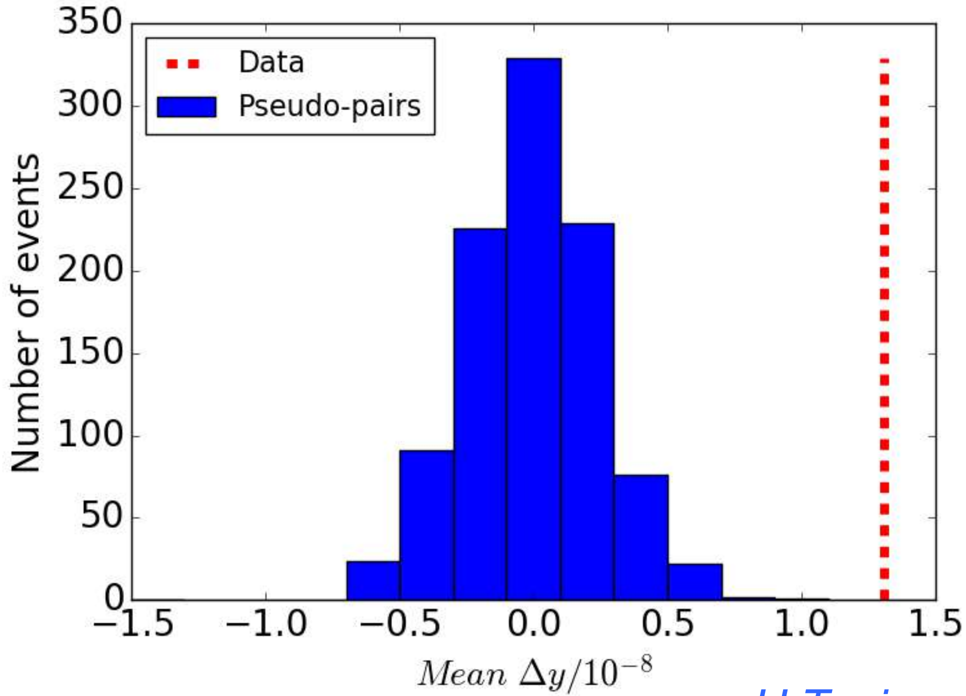

$$\Delta y = (1.31 \pm 0.25) \times 10^{-8}$$

$$5.3\sigma$$

*H Tanimura, …, **YZM**,… et al. 2018, MNRAS, 483, 223*

$$y = \int n_{\mathrm{e}} \sigma_{\mathrm{T}} \frac{k_{\mathrm{B}} T_{\mathrm{e}}}{m_{\mathrm{e}} c^2} \mathrm{d}l$$

$$n_{\mathrm{e}} = \overline{n}_{\mathrm{e,i}} (1 + \delta)$$

$$\overline{n}_{\mathrm{e,i}} = \frac{\chi \rho_{\mathrm{b}}(z)}{\mu_{\mathrm{e}} m_{\mathrm{p}}} \qquad \chi = \frac{1 - Y_{\mathrm{p}}(1 - N_{\mathrm{H_e}}/2)}{1 - Y_{\mathrm{p}}/2}$$

↓

$$\delta_c \left(\frac{T_{\mathrm{e}}}{10^7\ \mathrm{K}} \right) \left(\frac{r_c}{0.5 h^{-1}\ \mathrm{Mpc}} \right) = 2.7 \pm 0.5$$

H Tanimura, …, **YZM**,… et al. 2018, MNRAS, 483, 223

Same technique, but applied to **21-cm intensity mapping** (Parkes data)

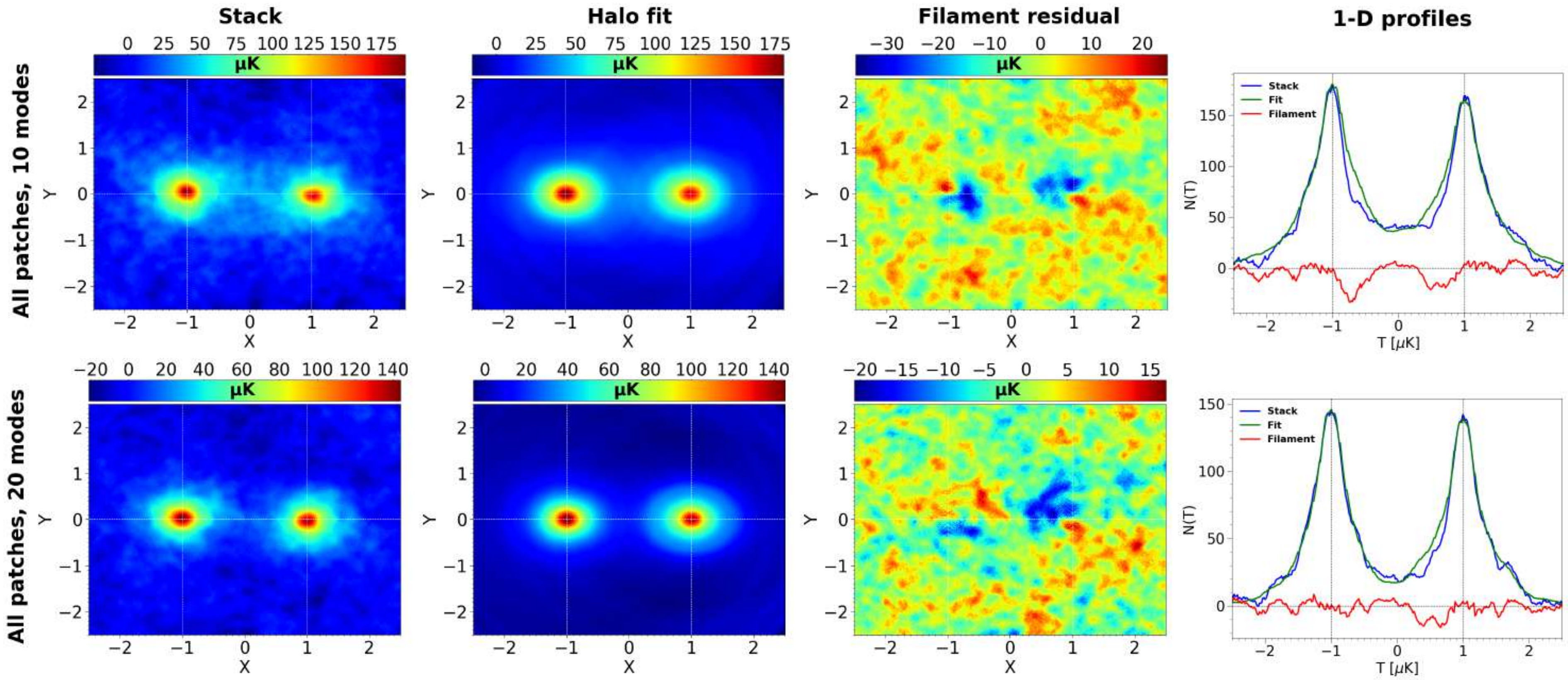

	T_b [μK]	$\Omega_{HI}^{(f)}$ [10^{-5}]	$x_{HI}\,\delta_b$ [10^{-4}]	N_{HI} [10^{15} cm^{-2}]
10 modes	$\lesssim 10.3$	$\lesssim 7.0$	$\lesssim 8.2$	$\lesssim 4.6$
20 modes	$\lesssim 4.8$	$\lesssim 3.2$	$\lesssim 3.8$	$\lesssim 2.1$

*D. Tramonte, **YZM**, Y.C. Li, L. Staveley-Smith, 2019, MNRAS*

thermal Sunyaev-Zeldovich effect X Weak Lensing

YZM, L. Van Waerbeke et al., 2015, JCAP, 09, 046
A. Hojjati, I. McCarthy, J. Harnois-Deraps, YZM et al., 2015, JCAP, 10, 047
A. Hojjati, …. , YZM,… 2017, JCAP, 471, 1565

Thermal SZ maps X Luminous red galaxies

H Tanimura, …, YZM,… et al. 2018, MNRAS, 483, 223

—>HI (21-cm) intensity mapping X Central galaxies

D. Tramonte, YZM, Y.C. Li, L. Staveley-Smith, 2019, MNRAS

kinetic Sunyaev-Zeldovich effect X **Peculiar velocity field**

Planck intermediate results XXXVII, 2016, A&A, 586, 140
C.Hernandez-Monteagudo, YZM, F-S Kitaura, W.Wang et al., 2015, Phys. Rev. Lett. 115, 191301
Yi-Chao Li, YZM, Mathieu Remazeilles, Kavilan Moodley, 2018, PRD, 97, 023514

kinetic SZ effect X MCXC clusters

Planck intermediate results LIII, 2018, A&A, 617, A48

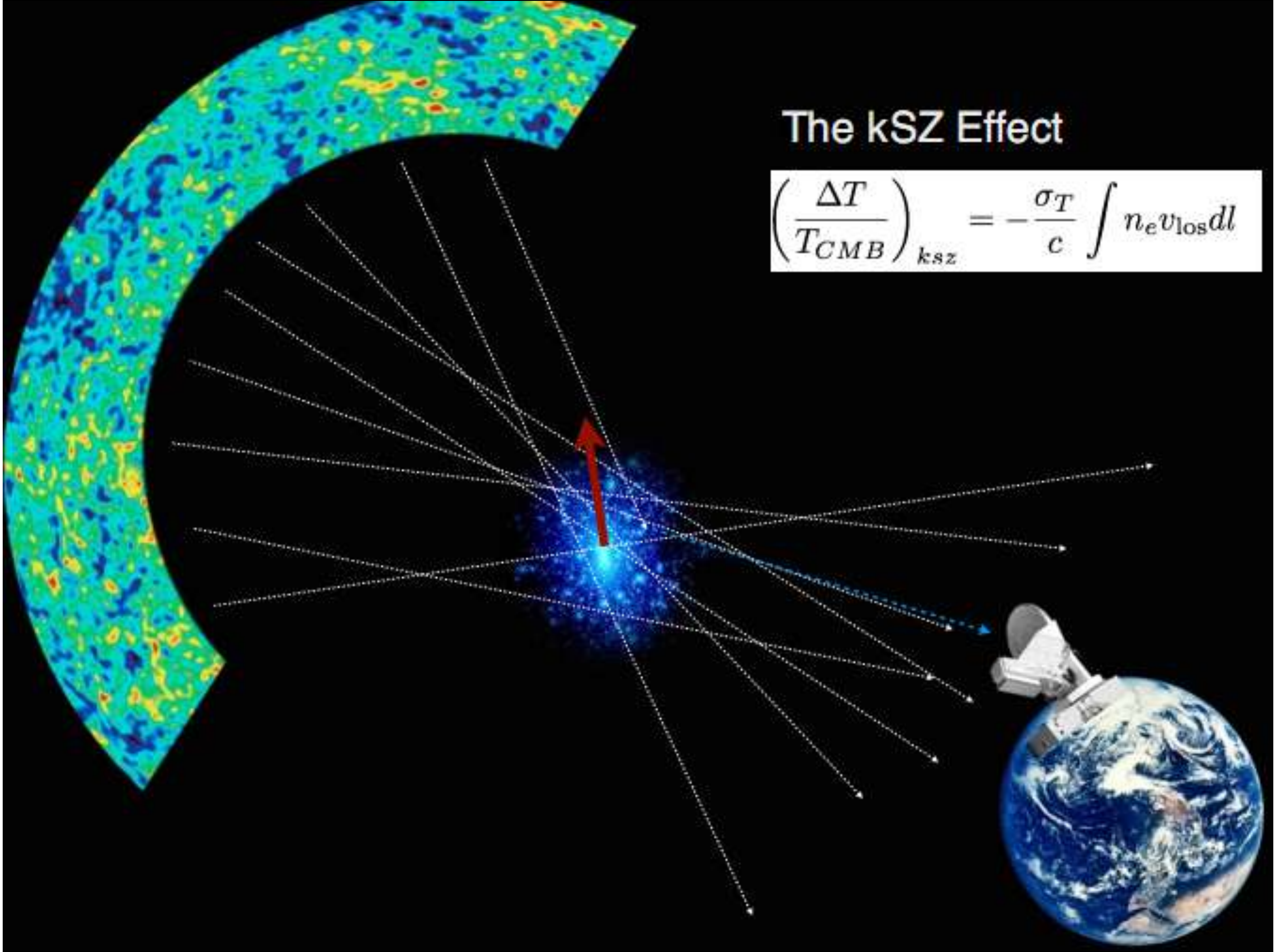
The kSZ Effect
$\left(\frac{\Delta T}{T_{CMB}}\right)_{ksz} = -\frac{\sigma_T}{c}\int n_e v_{\rm los} dl$

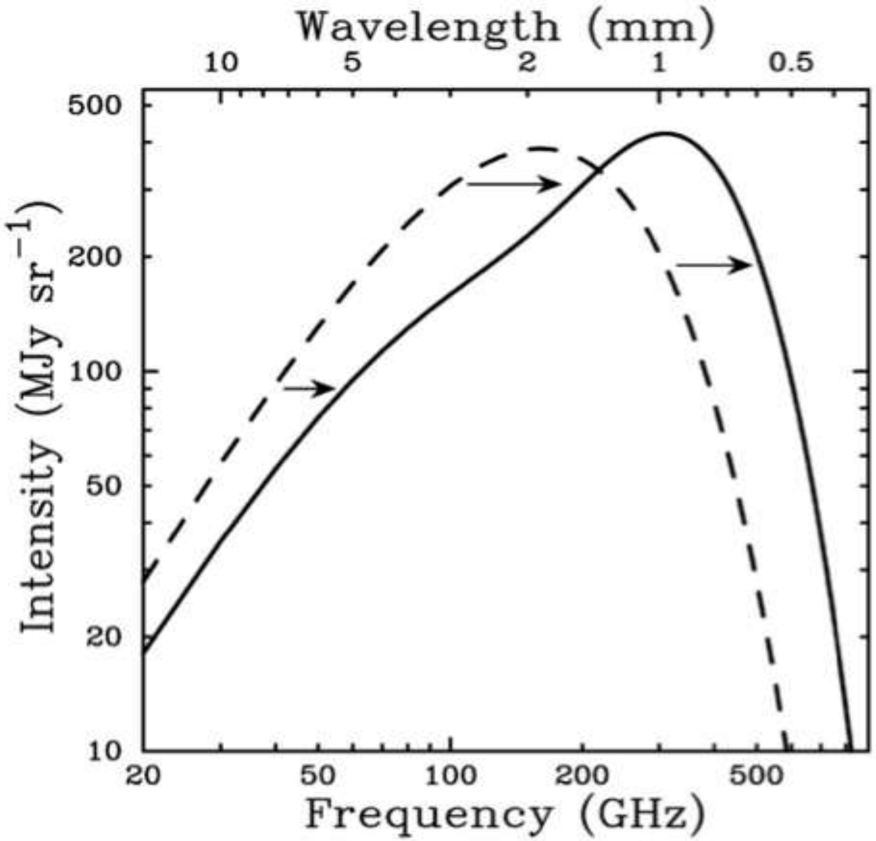

tSZ: $$\frac{\Delta T}{T} = \left[\eta \frac{e^{\eta}+1}{e^{\eta}-1} - 4\right] y \equiv g_{\nu} y$$

$$g_{\nu} \equiv (\eta(e^{\eta}+1)/(e^{\eta}-1)) - 4$$

$$\eta = \frac{h\nu}{k_B T_{\mathrm{CMB}}} = \frac{h\nu_0}{k_B T_0} = 1.76\left(\frac{\nu_0}{100\mathrm{GHz}}\right)$$

$$y = \frac{k_B \sigma_T}{m_e c^2} \int_0^l T_e(l) n_e(l)\, \mathrm{d}l$$

kSZ: $$\frac{\delta T}{T_0}(\hat{\boldsymbol{n}}) = -\int \mathrm{d}l\, \sigma_{\mathrm{T}} n_{\mathrm{e}} \left(\frac{\boldsymbol{v}}{c} \cdot \hat{\boldsymbol{n}}\right)$$

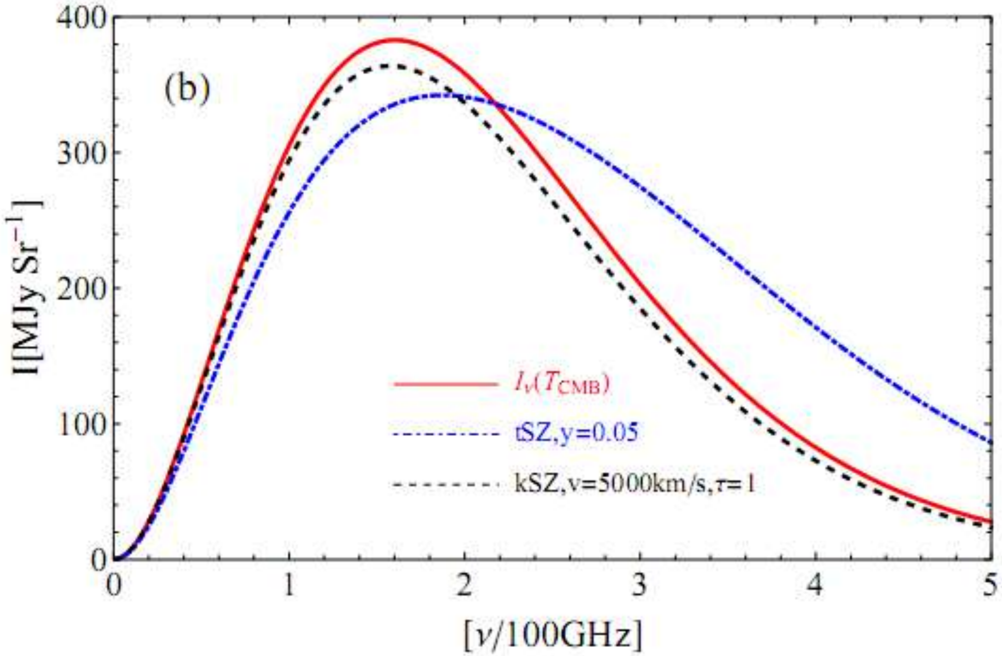

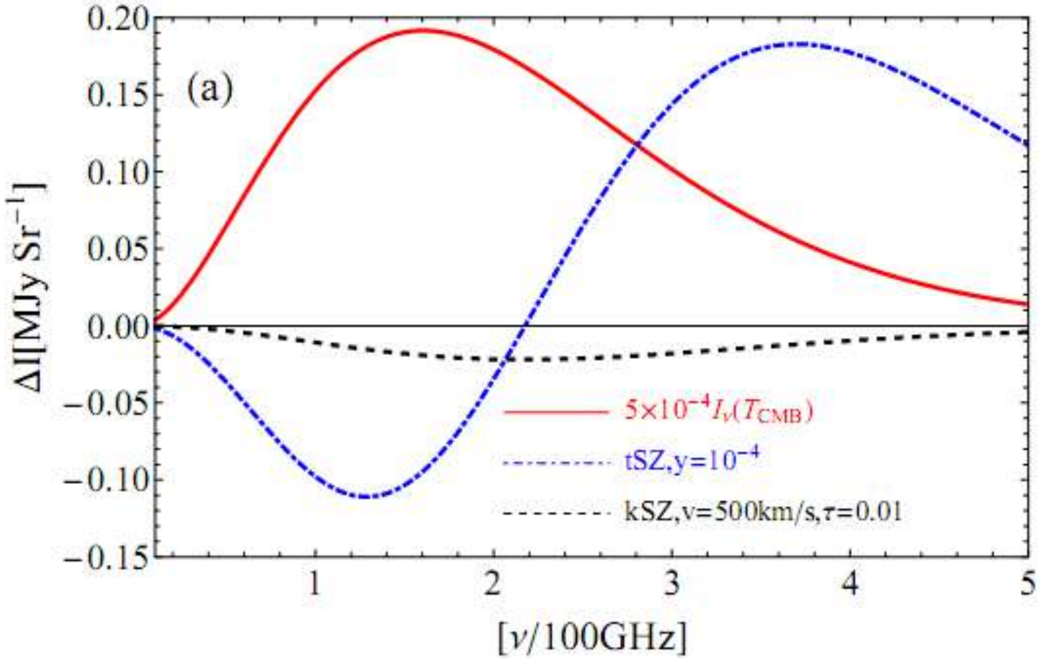

Planck SMICA, SEVEM, NILC maps

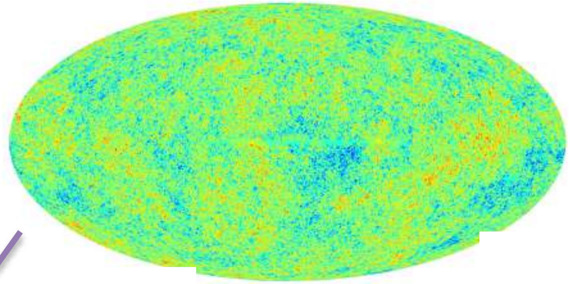

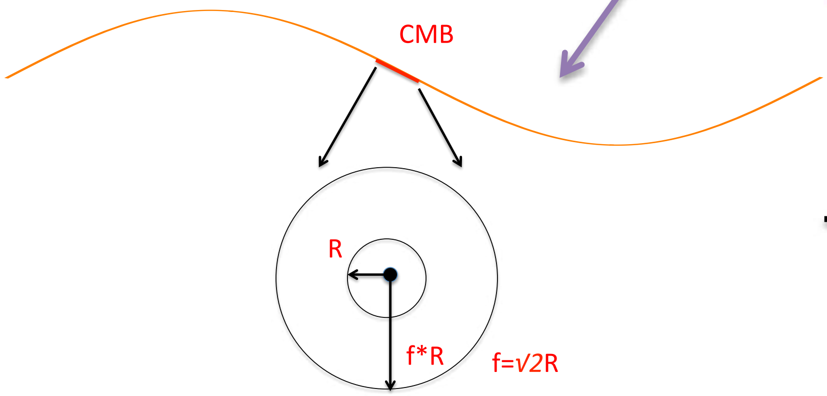

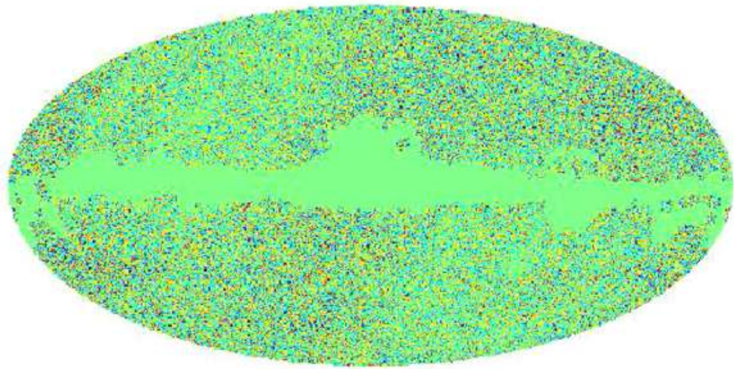

X

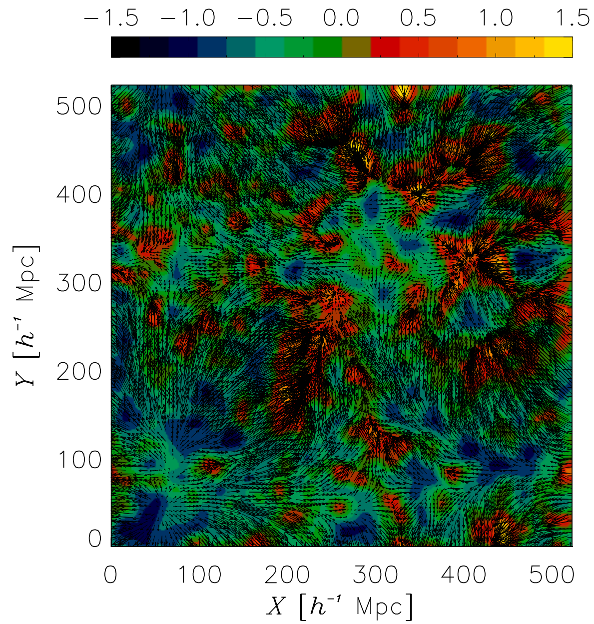

$$w^{T,v}(r) = \langle \delta T_i v_{\rm los}^{\rm rec}(\boldsymbol{x}_j) \rangle_{i,j}(r)$$

Planck SMICA, SEVEM, NILC maps

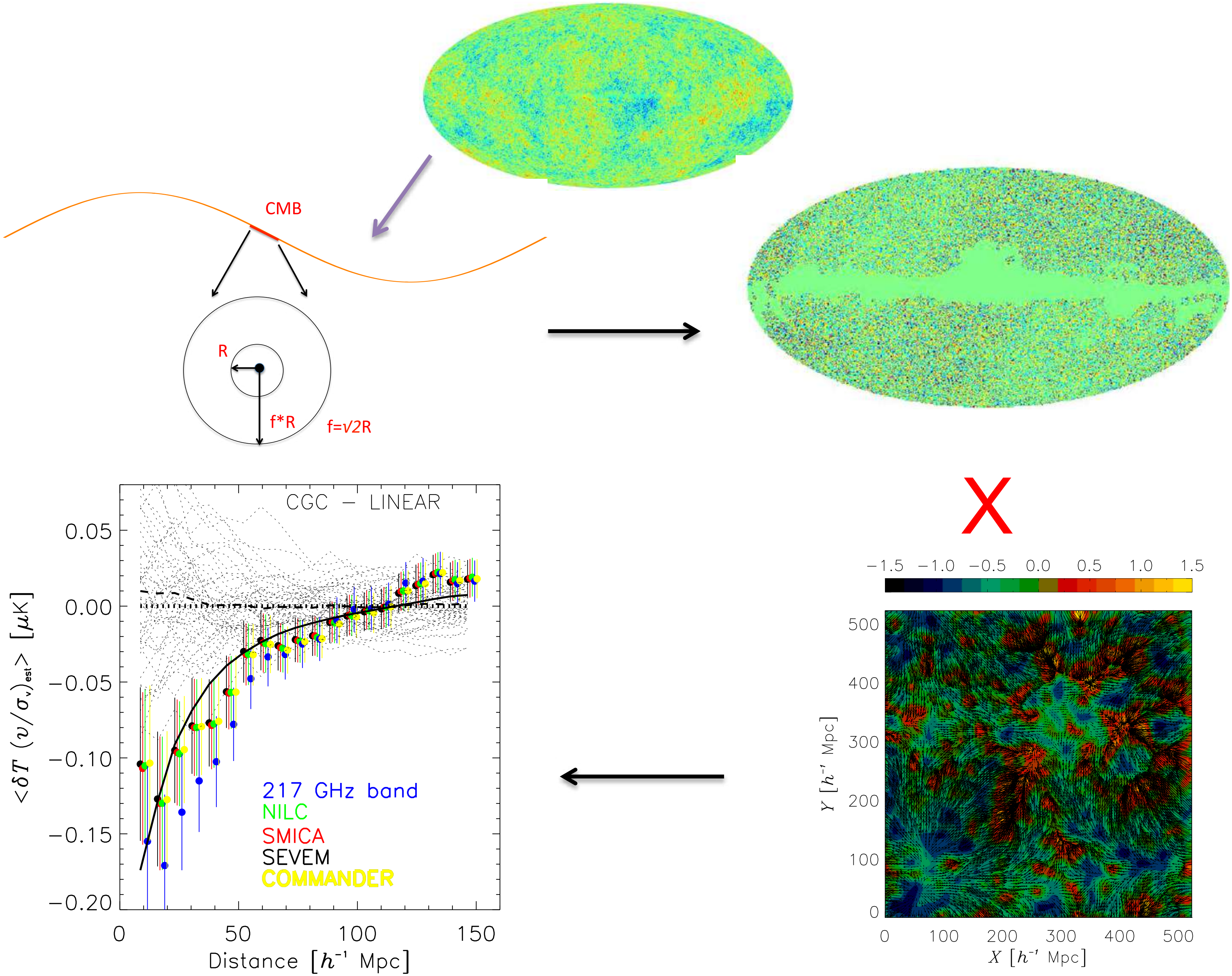

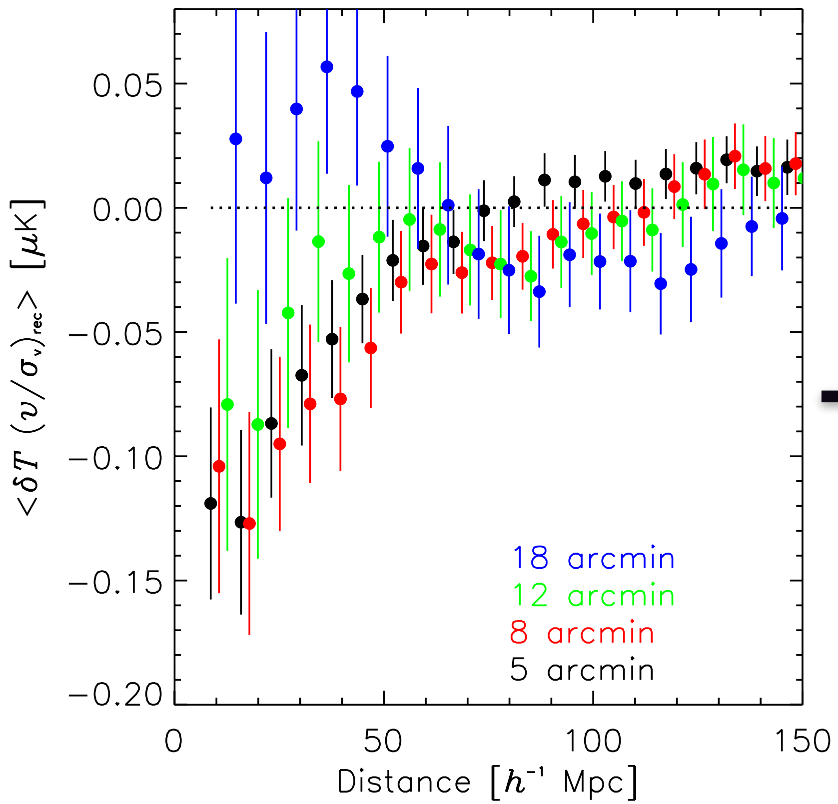

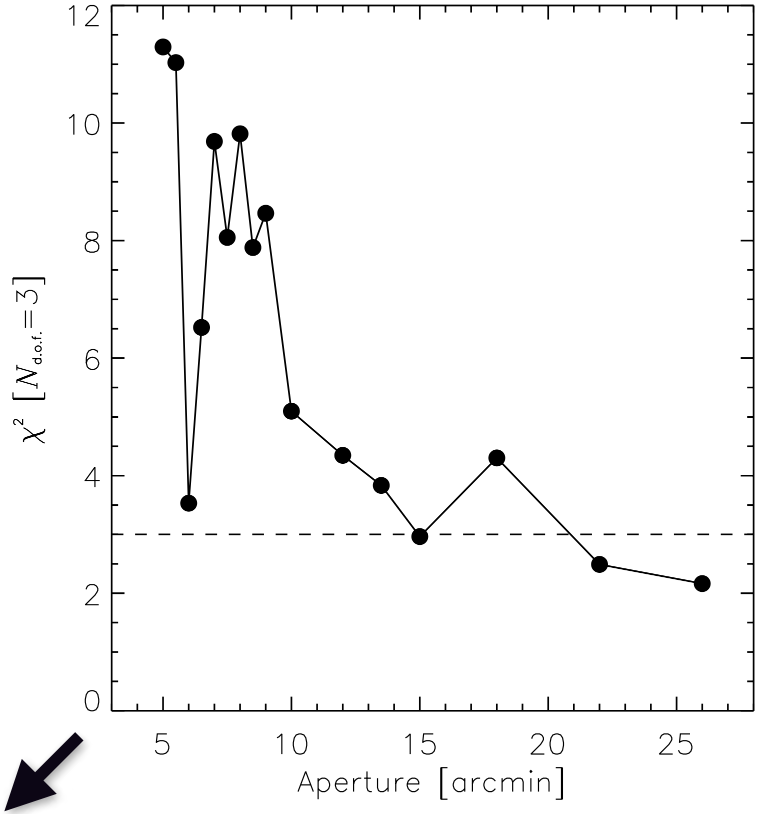

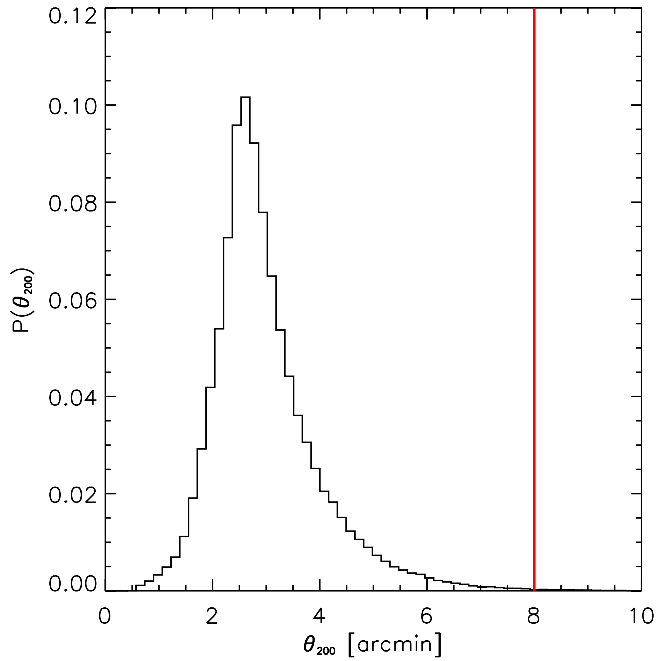

Planck intermediate results XXXVII, 2016, A&A, 586, 140

*C.Hernandez-Monteagudo, **YZM**, F-S Kitaura, W.Wang et al., 2015, Phys. Rev. Lett. 115, 191301*

Pairwise kSZ signal

$$\hat{p}_{\mathrm{kSZ}}(r) = -\frac{\sum_{i<j}(\delta T_{\mathrm{kSZ},i} - \delta T_{\mathrm{kSZ},j})c_{ij}}{\sum_{i<j} c_{ij}^2}$$

$$c_{ij} = \frac{(r_i - r_j)(1+\cos\theta)}{2\sqrt{r_i^2 + r_j^2 - 2 r_i r_j \cos\theta}}$$

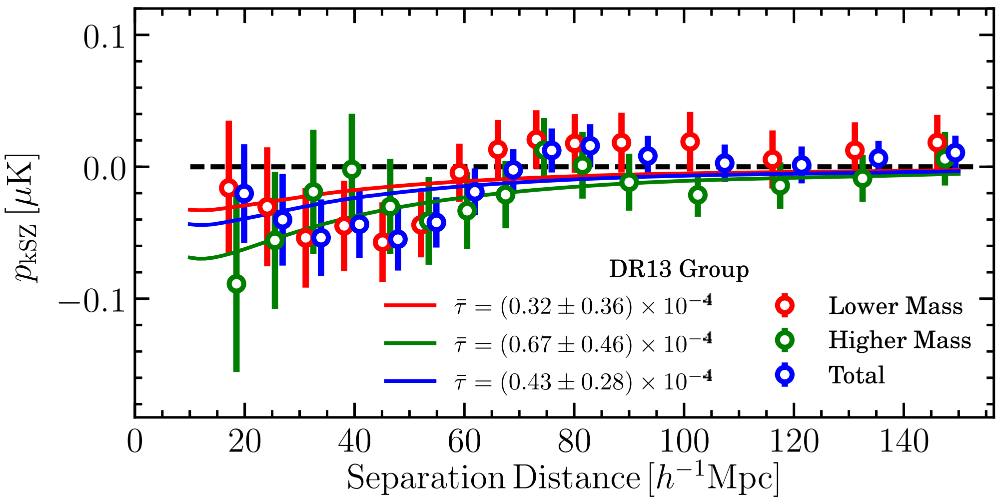

$\bar{\tau} = (0.53 \pm 0.32) \times 10^{-4} (1.65\sigma)$ LowZ North CGC;

$\bar{\tau} = (0.30 \pm 0.57) \times 10^{-4} (0.53\sigma)$ LowZ South CGC;

$\bar{\tau} = (0.43 \pm 0.28) \times 10^{-4} (1.53\sigma)$ DR13 Group.

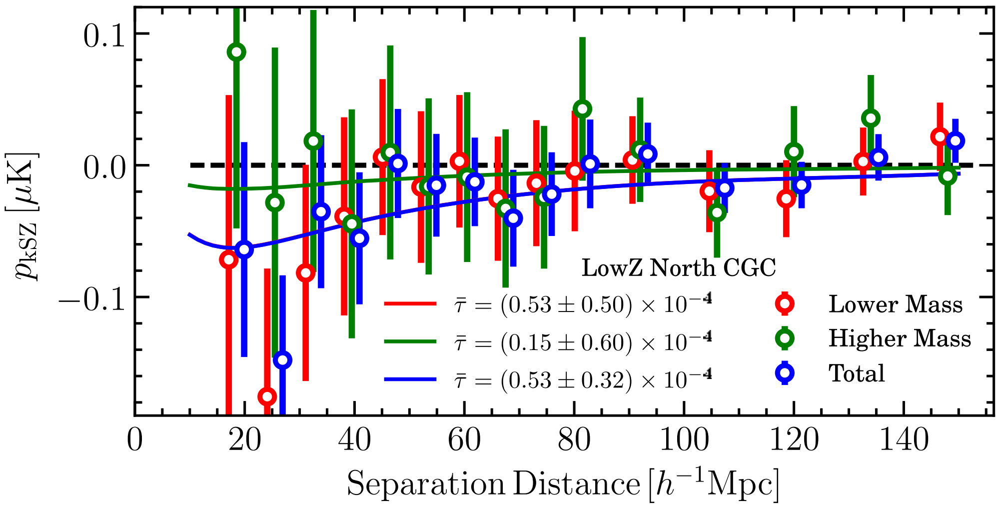

*Y.-C. Li, **YZM**, M. Remazeilles, K Moodley, 2018, PRD, 97, 023514*

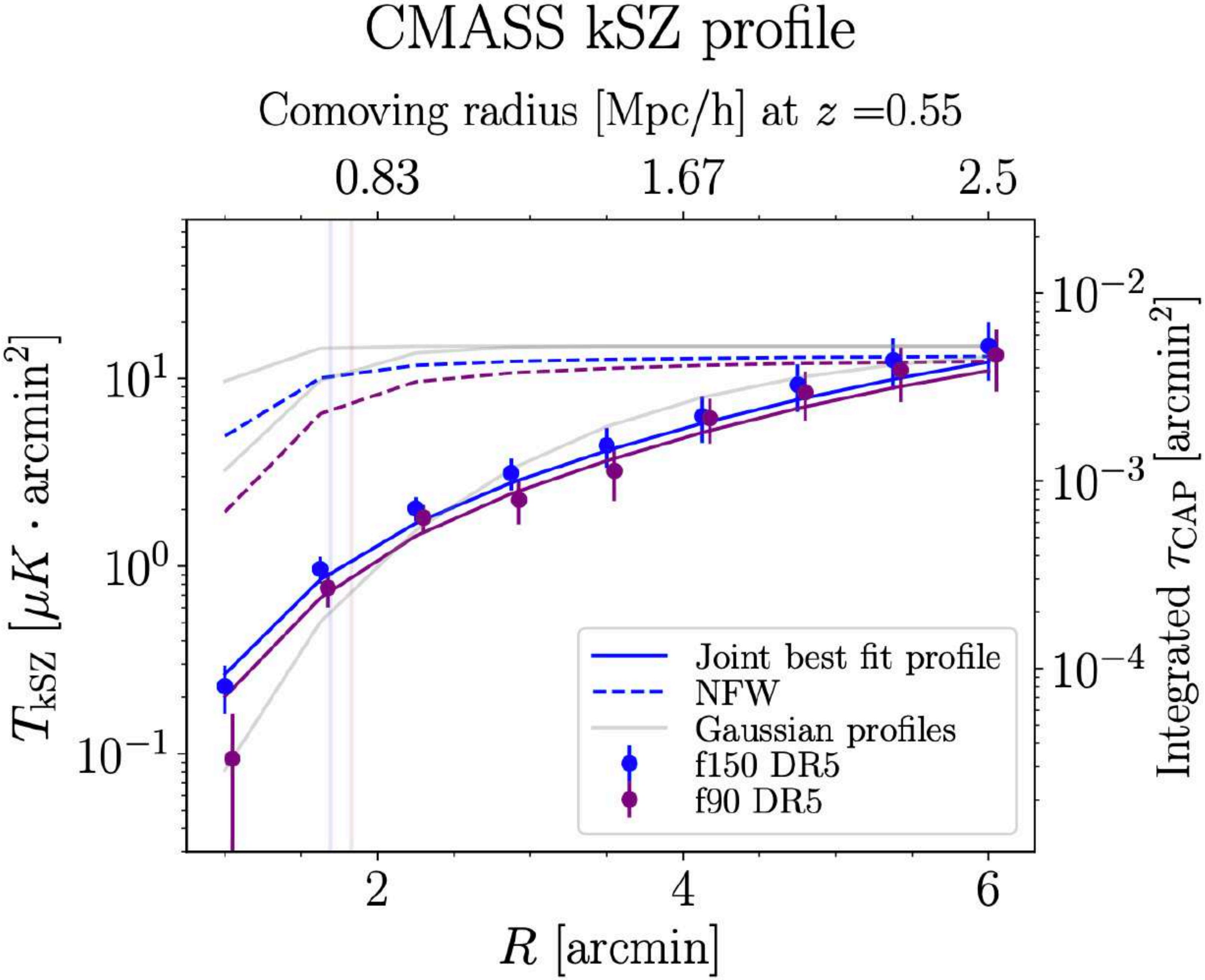

Atacama Cosmology Telescope 2020 results

thermal Sunyaev-Zeldovich effect X Weak Lensing

__YZM__, L. Van Waerbeke et al., 2015, JCAP, 09, 046
A. Hojjati, I. McCarthy, J. Harnois-Deraps, __YZM__ et al., 2015, JCAP, 10, 047
A. Hojjati, …. , __YZM__,… 2017, JCAP, 471, 1565

Thermal SZ maps X Luminous red galaxies

H Tanimura, …, __YZM__,… et al. 2018, MNRAS, 483, 223

—>HI (21-cm) intensity mapping X Central galaxies

D. Tramonte, __YZM__, Y.C. Li, L. Staveley-Smith, 2019, MNRAS

kinetic Sunyaev-Zeldovich effect X Peculiar velocity field

Planck intermediate results XXXVII, 2016, A&A, 586, 140
C.Hernandez-Monteagudo, __YZM__, F-S Kitaura, W.Wang et al., 2015, Phys. Rev. Lett. 115, 191301
Yi-Chao Li, __YZM__, Mathieu Remazeilles, Kavilan Moodley, 2018, PRD, 97, 023514

kinetic SZ effect X MCXC clusters

Planck intermediate results LIII, 2018, A&A, 617, A48

Method	Reference	kSZ data	Tracer type	Tracer data	Significance
Pairwise temperature difference	Hand et al. (2012)[a]	ACT	Galaxies (spec-z)	BOSS III/DR9	$2.9\,\sigma$
	Planck Collaboration Int. XXXVII (2016)	*Planck*	Galaxies (spec-z)	SDSS/DR7	1.8–$2.5\,\sigma$
	Hernández-Monteagudo et al. (2015)	*WMAP*	Galaxies (spec-z)	SDSS/DR7	$3.3\,\sigma$
	Soergel et al. (2016)	SPT	Clusters (photo-z)	1-yr DES	$4.2\,\sigma$
	De Bernardis et al. (2017)	ACT	Galaxies (spec-z)	BOSS/DR11	3.6–$4.1\,\sigma$
	Sugiyama et al. (2017)[b]	*Planck*	Galaxies (spec-z)	BOSS/DR12	$2.45\,\sigma$
	Li et al. (2018)[b]	*Planck*	Galaxies (spec-z)	BOSS/DR12	$1.65\,\sigma$
kSZ × $v_{\rm pec}$	Planck Collaboration Int. XXXVII (2016)[c]	*Planck*	Galaxy velocities	SDSS/DR7	3.0–$3.7\,\sigma$
	Schaan et al. (2016)[c]	ACT	Galaxy velocities	BOSS/DR10	$2.9\,\sigma$, $3.3\,\sigma$
kSZ^2 × projected density field	Hill et al. (2016), [illegible] (2016)[d]	*Planck*, *WMAP*	Projected overdensities	WISE catalogue	3.8–$4.5\,\sigma$
kSZ dispersion	Planck Collaboration Int. LIII (2018)	*Planck*	Clusters	MCXC	$2.8\,\sigma$

Planck intermediate results

LIII. Detection of velocity dispersion from the kinetic Sunyaev-Zeldovich effect

Planck Collaboration: N. Aghanim[48], Y. Akrami[50,51], M. Ashdown[58,4], J. Aumont[83], C. Baccigalupi[70], M. Ballardini[17,35], A. J. Banday[83,7], R. B. Barreiro[53], N. Bartolo[23,54], S. Basak[75], R. Battye[56], K. Benabed[49,82], J.-P. Bernard[83,7], M. Bersanelli[26,39], P. Bielewicz[68,7,70], J. R. Bond[6], J. Borrill[9,80], F. R. Bouchet[49,77], C. Burigana[38,24,41], E. Calabrese[73], J. Carron[18], H.C. Chiang[20,5], B. Comis[61], D. Contreras[16], B. P. Crill[55,8], A. Curto[53,4,58], F. Cuttaia[35], P. de Bernardis[25], A. de Rosa[35], G. de Zotti[36,70], J. Delabrouille[1], E. Di Valentino[49,77], C. Dickinson[56], J. M. Diego[53], O. Doré[55,8], A. Ducout[49,47], X. Dupac[29], F. Elsner[65], T. A. Enßlin[65], H. K. Eriksen[51], E. Falgarone[60], Y. Fantaye[2,15], F. Finelli[35,41], F. Forastieri[24,42], M. Frailis[37], A. A. Fraisse[20], E. Franceschi[35], A. Frolov[76], S. Galeotta[37], S. Galli[57], K. Ganga[1], M. Gerbino[81,69,25], K. M. Górski[55,84], A. Gruppuso[35,41], J. E. Gudmundsson[81,20], W. Handley[58,4], F. K. Hansen[51], D. Herranz[53], E. Hivon[49,82], Z. Huang[74], A. H. Jaffe[47], E. Keihänen[19], R. Keskitalo[9], K. Kiiveri[19,34], J. Kim[65], T. S. Kisner[63], N. Krachmalnicoff[70], M. Kunz[11,48,2], H. Kurki-Suonio[19,34], J.-M. Lamarre[60], A. Lasenby[4,58], M. Lattanzi[24,42], C. R. Lawrence[55], M. Le Jeune[1], F. Levrier[60], M. Liguori[23,54], P. B. Lilje[51], V. Lindholm[19,34], M. López-Caniego[29], P. M. Lubin[21], Y.-Z. Ma[56,72,67,⋆], J. F. Macías-Pérez[61], G. Maggio[37], D. Maino[26,39,43], N. Mandolesi[35,24], A. Mangilli[7], P. G. Martin[6], E. Martínez-González[53], S. Matarrese[23,54,31], N. Mauri[41], J. D. McEwen[66], A. Melchiorri[25,44], A. Mennella[26,39], M. Migliaccio[79,45], M.-A. Miville-Deschênes[48,6], D. Molinari[24,35,42], A. Moneti[49], L. Montier[83,7], G. Morgante[35], P. Natoli[24,79,42], C. A. Oxborrow[10], L. Pagano[48,60], D. Paoletti[35,41], B. Partridge[33], O. Perdereau[59], L. Perotto[61], V. Pettorino[32], F. Piacentini[25], S. Plaszczynski[59], L. Polastri[24,42], G. Polenta[3], J. P. Rachen[14], B. Racine[51], M. Reinecke[65], M. Remazeilles[56,48,1], A. Renzi[70,46], G. Rocha[55,8], G. Roudier[1,60,55], B. Ruiz-Granados[52,12], M. Sandri[35], M. Savelainen[19,34,64], D. Scott[16], C. Sirignano[23,54], G. Sirri[41], L. D. Spencer[73], L. Stanco[54], R. Sunyaev[65,78], J. A. Tauber[30], D. Tavagnacco[37,27], M. Tenti[40], L. Toffolatti[13,35], M. Tomasi[26,39], M. Tristram[59], T. Trombetti[38,42], J. Valiviita[19,34], F. Van Tent[62], P. Vielva[53], F. Villa[35], N. Vittorio[28], B. D. Wandelt[49,82,22], I. K. Wehus[55,51], A. Zacchei[37], and A. Zonca[71]

(Affiliations can be found after the references)

Received 2 July 2017 / Accepted 12 June 2018

⋆ Corresponding author: Y.-Z. Ma, ma@ukzn.ac.za

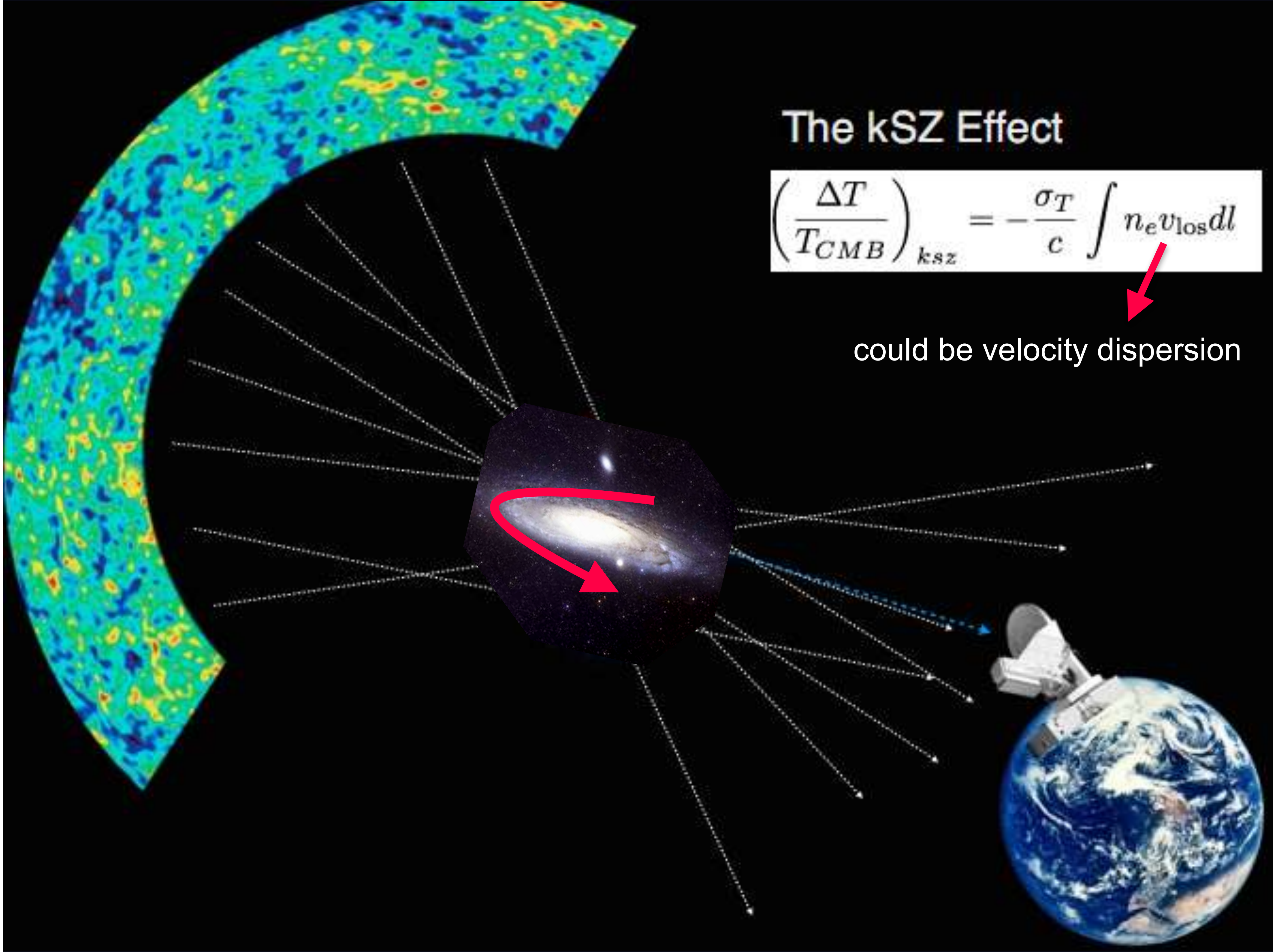
The kSZ Effect
$\left(\frac{\Delta T}{T_{CMB}}\right)_{ksz} = -\frac{\sigma_T}{c}\int n_e v_{\rm los} dl$
could be velocity dispersion

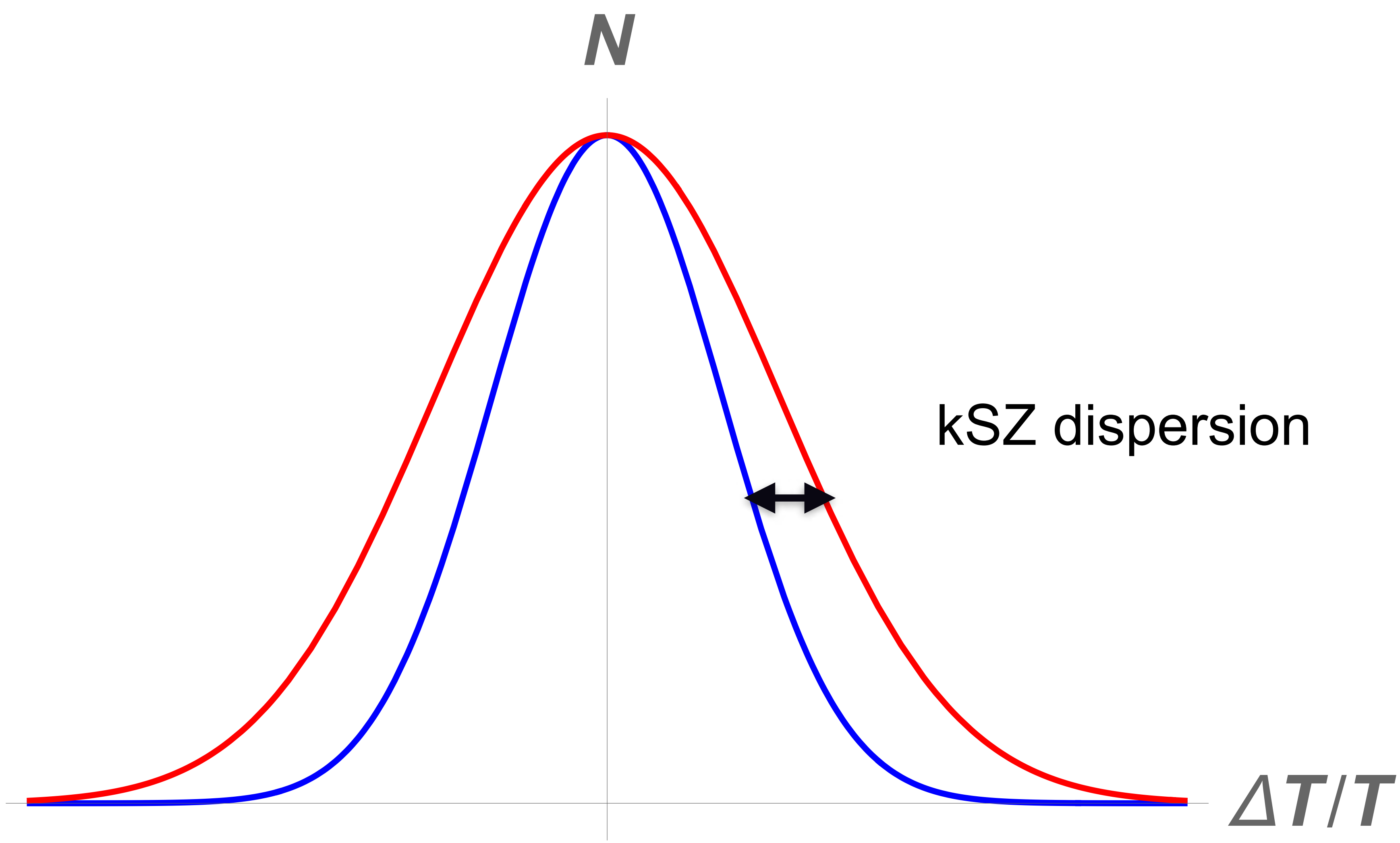

As an analogical example, the average cancer rate above age 60 is N_1, and for some particular region, some extra condition (unhealthy diet or lifestyle/smoke/stress/poor living condition etc) can boost it up to N_2 ($N_2 > N_1$), the excess rate $N_2 - N_1$ is due to the “extra condition”.

Global filter:

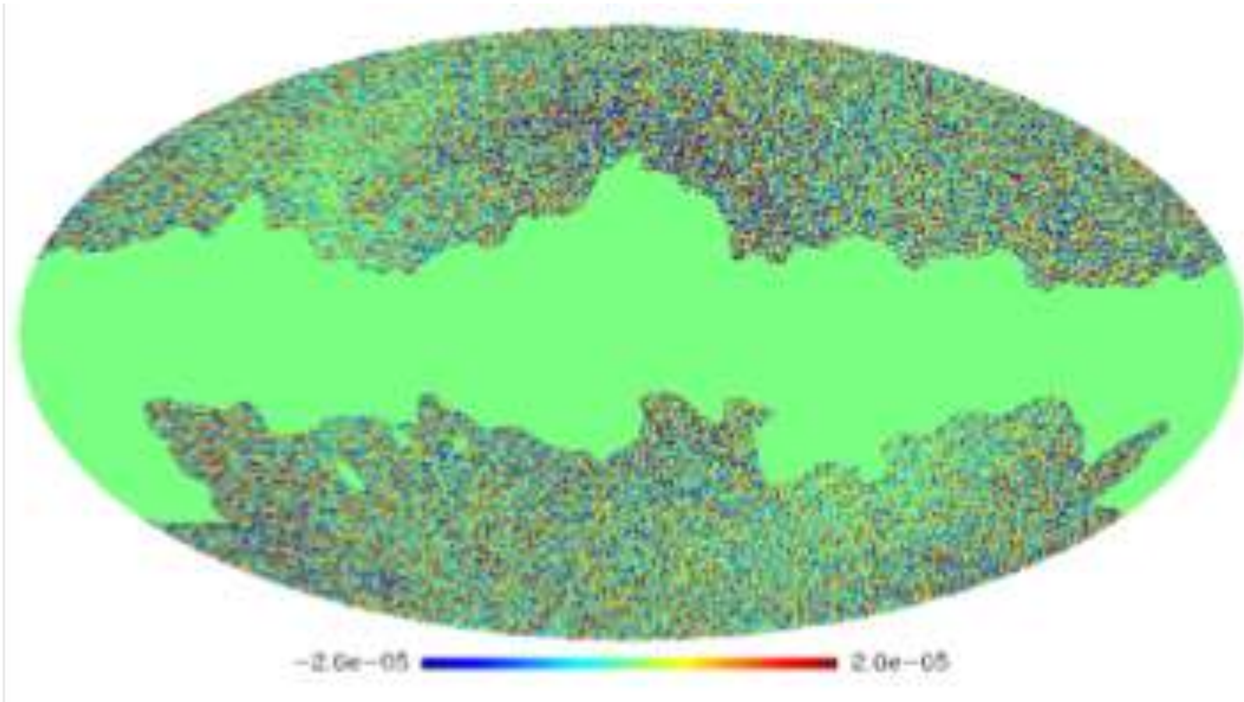

$$W_\ell = \frac{B_\ell}{B_\ell^2 C_\ell^{\rm CMB} + N_\ell} = \frac{B_\ell}{C_\ell^{\rm noise}}$$

1526 MCXC clusters outside Galactic mask

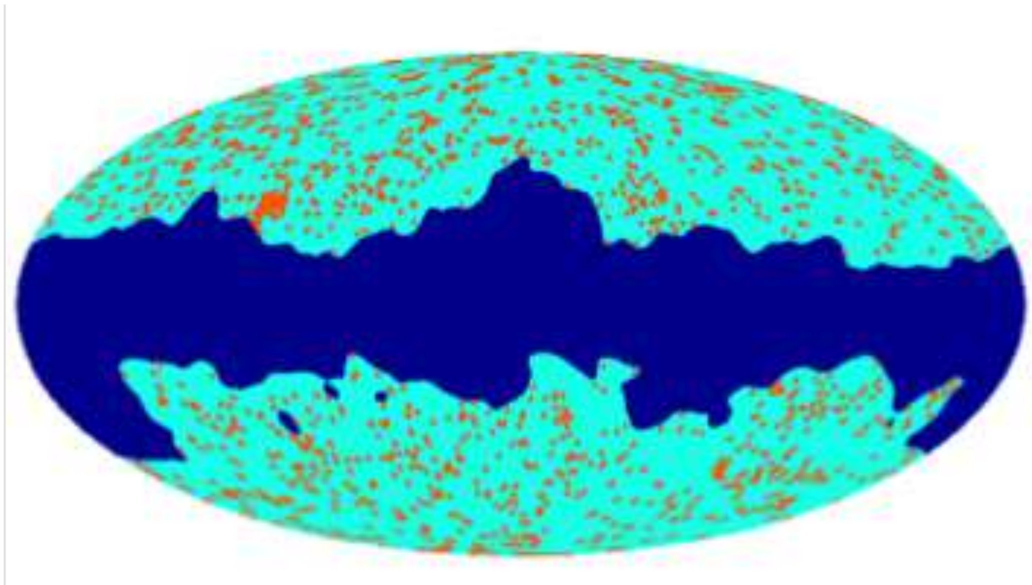

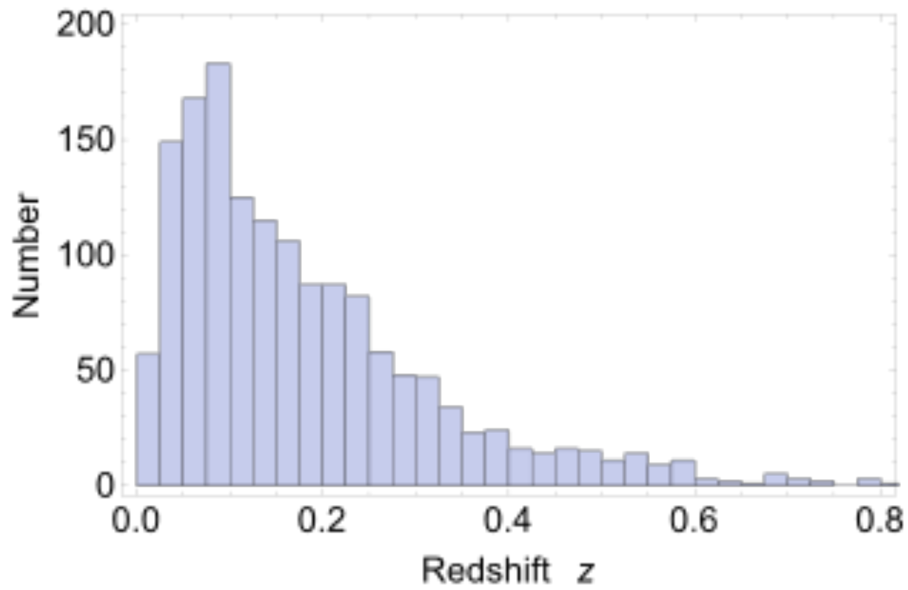

	True positions	Random positions
Mean	−0.015	−0.021
Variance	1.38	1.23
Skewness	0.37	0.09
Kurtosis	4.44	3.29

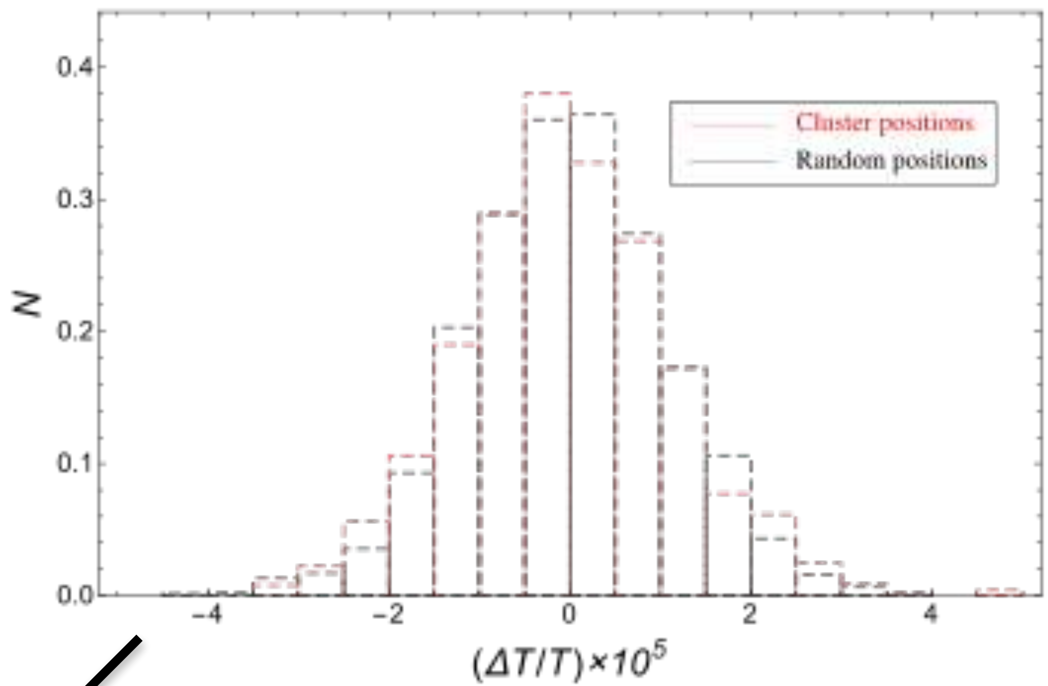

extract width

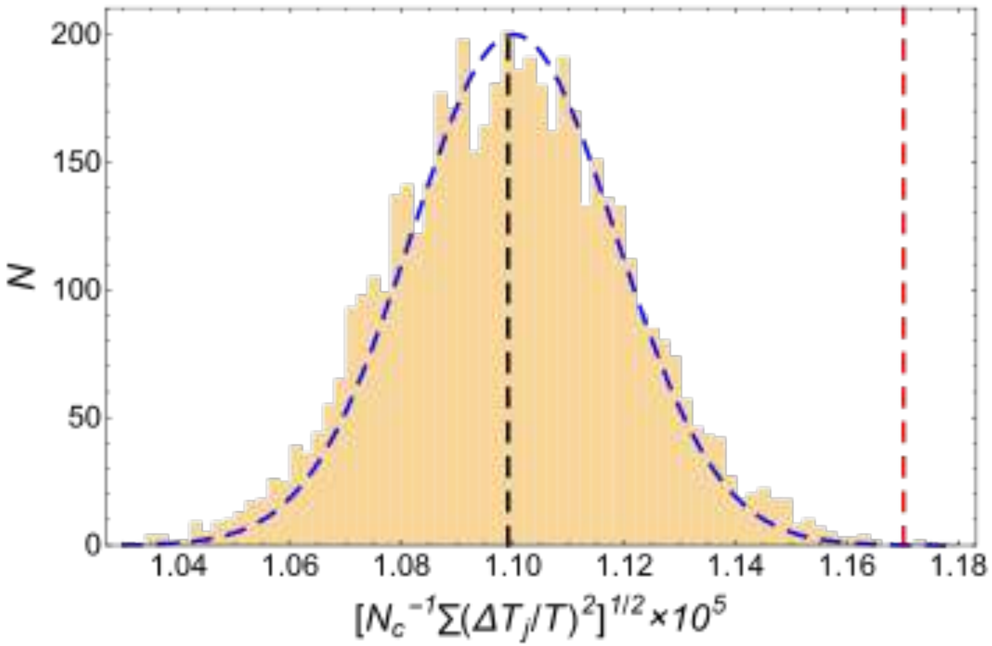

$$\widehat{s^2} = \frac{1}{N_c}\sum_i \delta_i^2 - \frac{1}{N_c}\sum_i \hat{n}_i^2$$

Map	$E[s^2] \times 10^{11}$	$(V[s^2])^{1/2} \times 10^{11}$	S/N
2D-ILC	1.64	0.48	3.4
SMICA	3.53	0.37	9.4
NILC	2.75	0.38	7.3
SEVEM	3.19	0.40	8.1
Commander	1.47	0.42	3.5

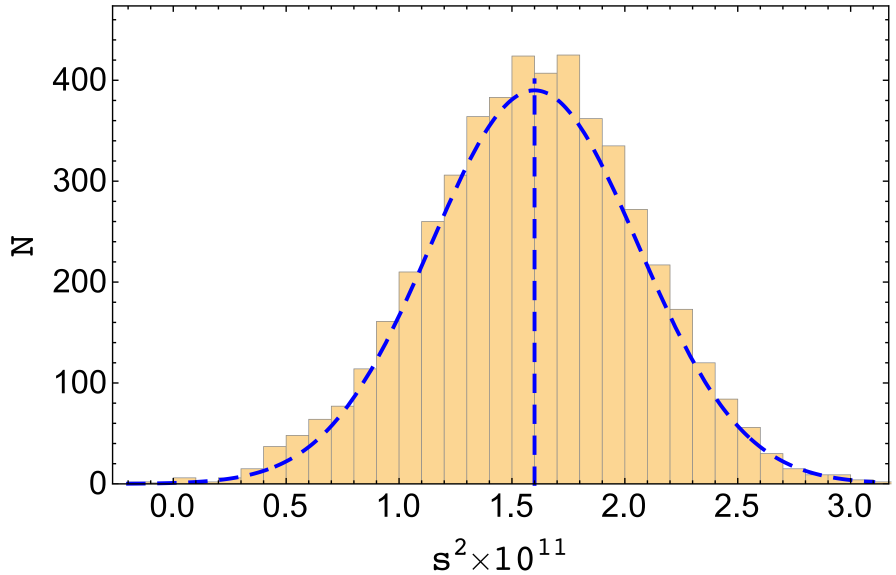

$$P(s_w^2 < 0) = 0.07\%$$

Corrected for lensing contribution:

$$\left(\widehat{s^2}\right) = (1.35 \pm 0.48) \times 10^{-11}$$

$$2.8\,\sigma$$

Planck intermediate results LIII, 2018, A&A, 617, A48

$$\langle v^2 \rangle = (123\,000 \pm 71\,000)\,(\mathrm{km\,s^{-1}})^2$$

$$= \left\langle \left(v_{\mathrm{bulk}} + v_{\mathrm{dis}}\right)^2 \right\rangle = \left\langle v_{\mathrm{bulk}}^2 \right\rangle + \sigma_{\mathrm{dis}}^2$$

Statistical homogeneity on 600 Mpc scale

Summary

- Most of the baryons are diffuse and warm-hot IGM with $T = 10^4 - 10^7\,\mathrm{K}$.

SZ data	LSS tracers	Results
thermal SZ	weak lensing	Gas extends out to $5r_{\mathrm{vir}}$, with temperature for $M = 10^{12} - 10^{16} \mathrm{M}_{\odot}$ consistent with simulation
thermal SZ	luminous red galaxies	Gas associated with filament is detected at $y = (1.31 \pm 0.25) \times 10^{-8}$ —> $T_{\mathrm{filament}} \leqslant 10^7\,\mathrm{K}$
kinetic SZ	(reconstructed) velocity field	Maximum detection is reached at $\theta_{\mathrm{AP}} = 8\,\mathrm{arcmin}$ which is $\sim 3r_{\mathrm{vir}}$
kinetic SZ	X-ray selected clusters	$\left\langle (\Delta T/T)^2 \right\rangle = (1.35 \pm 0.48) \times 10^{-11}$ The Universe is homogenous at 600 Mpc.

- Our results suggest that missing baryon at low redshifts is *not* missing, but correlated with underlying LSS density field.

Back to the general picture

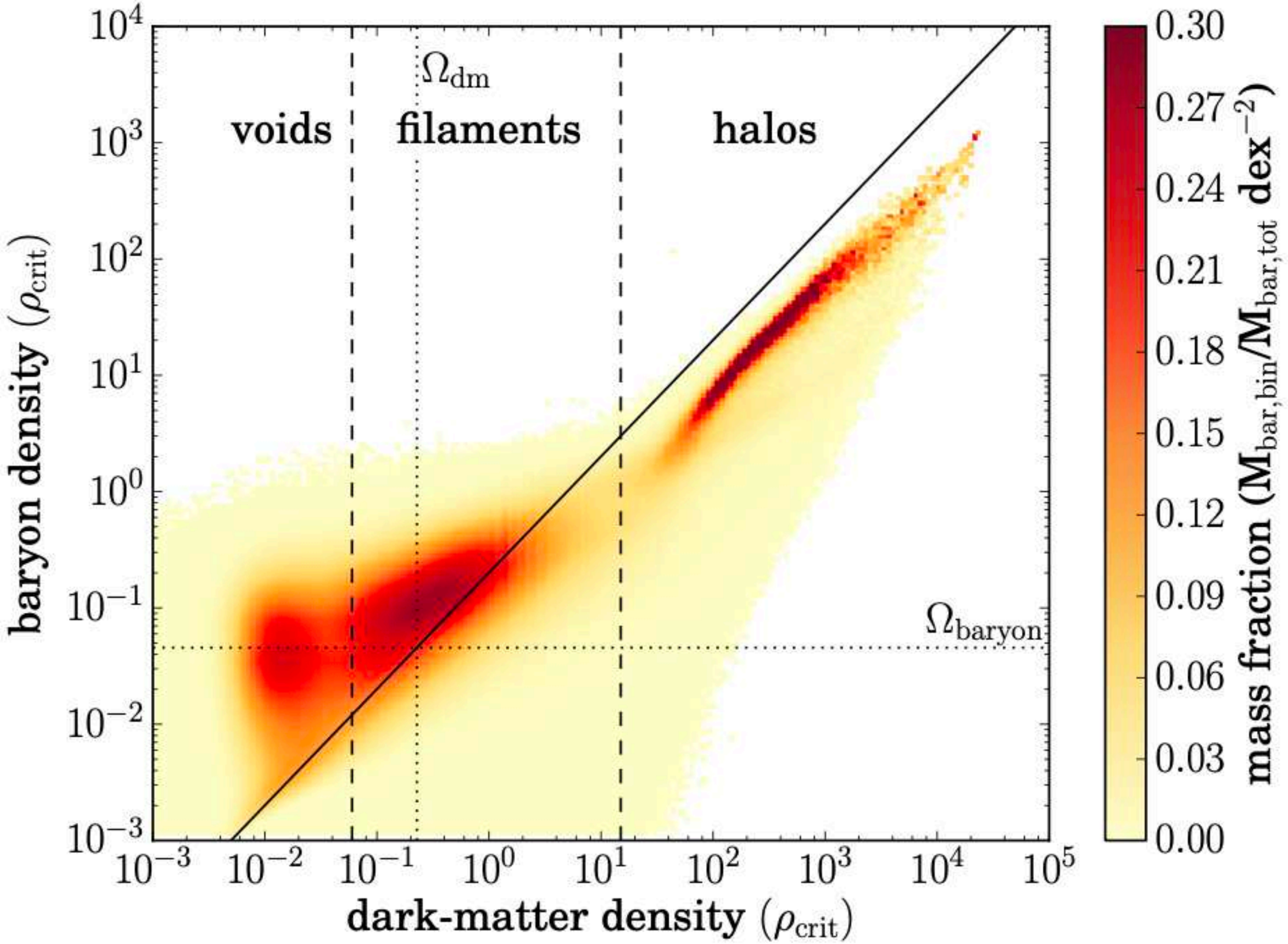

M. Haider et al. 2016, MNRAS

component	dark matter density region ($\rho_{\rm crit}$)	% of total dark matter mass	% of total baryonic mass	% of total mass	% of total volume
haloes	> 15	49.2 %	23.2 %	44.9 %	0.16 %
filaments	0.06 - 15	44.5 %	46.4 %	44.8 %	21.6 %
voids	0 - 0.06	6.4 %	30.4 %	10.4 %	78.2 %
ejected material inside voids	0 - 0.06	2.6 %	23.6 %	6.1 %	30.4 %

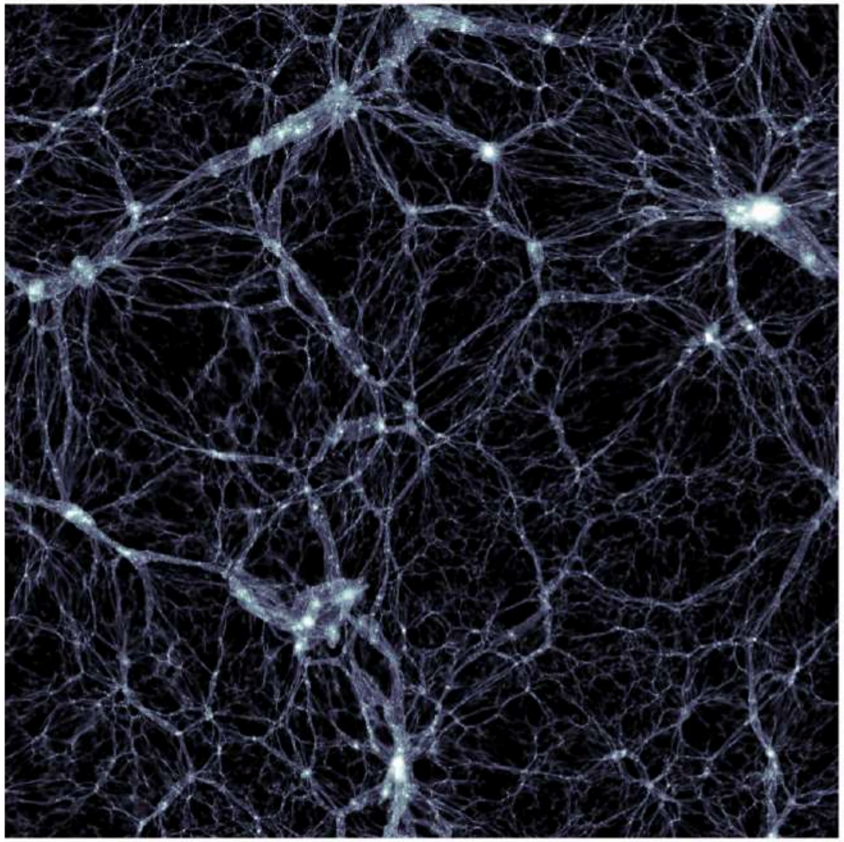

(a) dark matter

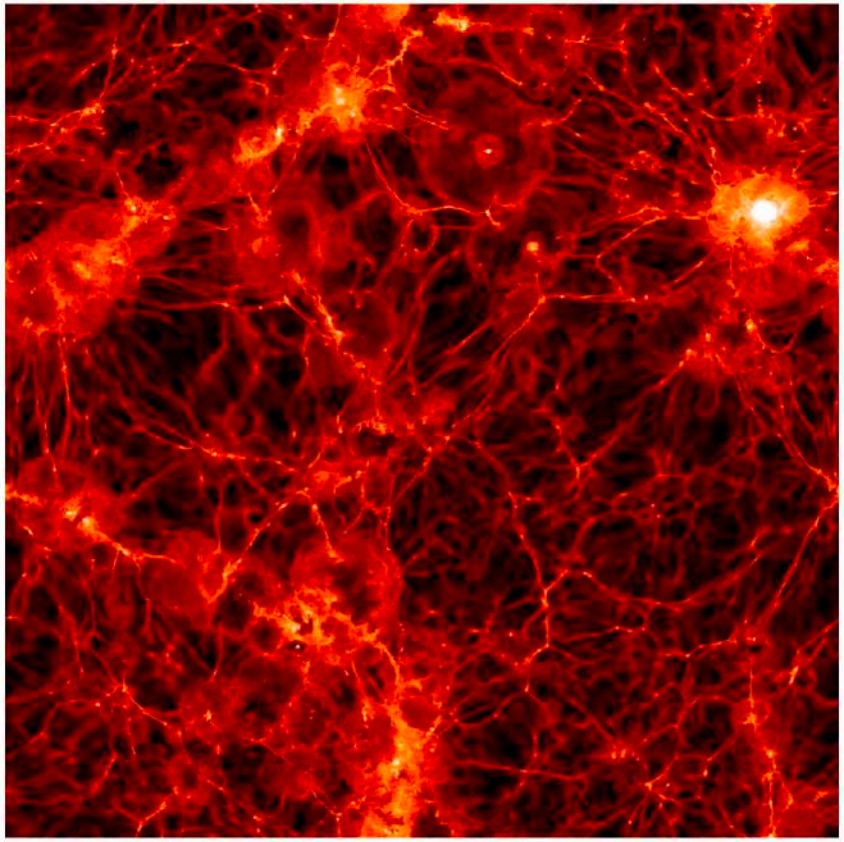

(b) baryons

Figure 3. Dark matter and baryon density in a thin slice at $z = 0$. The slice covers the whole $(106.5\ \mathrm{Mpc})^2$ extent of the simulation and has a thickness of 104 kpc (1 cell).

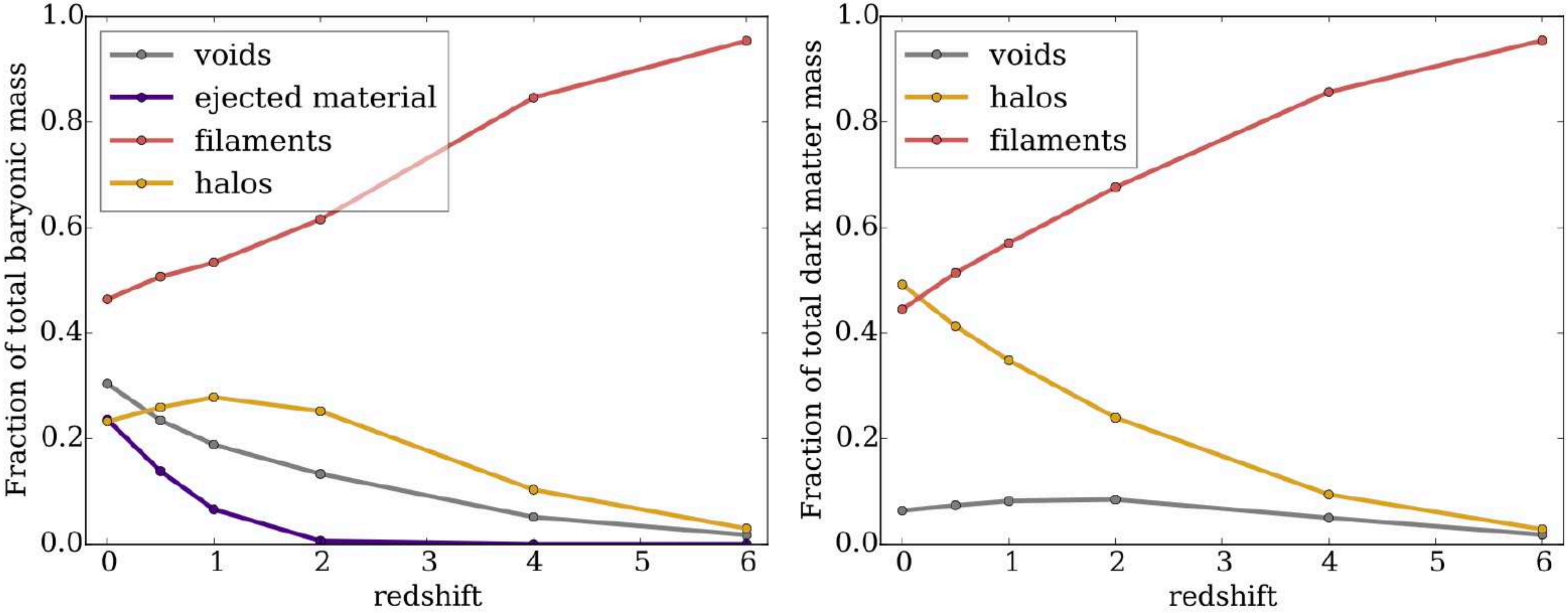

We should find higher baryon fractions in filaments and voids, but the latter is extremely difficult to measure. But with LSST + CMB-S4 experiments, the sky coverage will be as large as 6000 $\deg^2$, and very low CMB thermal noise and better angular resolution (~1 arcmin), which has a strong potential to disentangle the signal from filaments and voids.